CASCADE DESIGN OF SINGLE INPUT SINGLE OUTPUT SYSTEMS USING H_∞ AND QUANTITATIVE FEEDBACK THEORY METHODOLOGIES

A Thesis

by

MAYANK LAL

Submitted to the Office of Graduate Studies of
Texas A&M University
in partial fulfillment of the requirements for the degree of

MASTER OF SCIENCE

December 2004

Major Subject: Mechanical Engineering

CASCADE DESIGN OF SINGLE INPUT SINGLE OUTPUT SYSTEMS USING H_∞ AND QUANTITATIVE FEEDBACK THEORY METHODOLOGIES

A Thesis

by

MAYANK LAL

Submitted to Texas A&M University
in partial fulfillment of the requirements
for the degree of

MASTER OF SCIENCE

Approved as to style and content by:

Suhada Jayasuriya (Chair of Committee)	Shankar P. Bhattacharyya (Member)
Alexander Parlos (Member)	Dennis O. Neal (Head of Department)

December 2004

Major Subject: Mechanical Engineering

ABSTRACT

Cascade Design of Single Input Single Output Systems Using H_∞

and Quantitative Feedback Theory Methodologies.

(December 2004)

Mayank Lal, B.Tech., IIT Kharagpur

Chair of Advisory Committee: Dr. Suhada Jayasuriya

This thesis considers the design of cascaded SISO control systems using the H_∞ and QFT methodologies. In the first part of the thesis the actual advantages offered by Single Input Single Output (SISO) cascade loop structures are studied. In Quantitative Feedback Theory(QFT) it is emphasized that the use of cascaded loops is primarily for the reduction of bandwidth of the controllers. This in turn helps in considerable reduction of the adverse effects of high frequency noise. The question that arises then is whether or not there are any substantial benefits to be gained by cascade loop design in the low frequencies. It is shown using QFT methodology that there aren't any advantages gained in the low frequencies with the use of cascaded design. In effect it is concluded that if the design is properly executed a single loop controller closed from the output to the input will be sufficient to meet the typical performance specifications. This is shown using an example where the mold level of a continuous casting process is to be controlled. The plant being used has considerable uncertainty so that features of robust control can be highlighted.

In the second part the Robust Outer Loop bounds were generated analytically and examined for certain properties. It was compared to the bounds generated by already existing algorithms.

In the third part the inner outer QFT design was modified with the inner loop being designed using H_∞ with the concept of sensitivity shaping. This design was very similar to the pure QFT design with the added advantage of having some automation.

In the fourth part the H_∞ methodology was used to design a two loop control structure. The idea was to compare this design to the QFT design. It was seen that H_∞ generated redundant controllers and pre filters.

ACKNOWLEDGEMENTS

I would like to express my gratitude to a number of people without whom it would have been impossible to complete this thesis. First of all, I would like to thank my advisor, Dr. Suhada Jayasuriya, for his guidance and support during the course of my research work. His stimulating suggestions were extremely helpful.

I am thankful to Elizabeth Villota for extending resources to me and sharing knowledge in the area of robust control.

I am thankful to Murray Kerr for reviewing my work and coming up with valuable suggestions. He was also very generous in sharing resources with me.

I am thankful to my parents and brothers for the immense support, encouragement and love without which it would have been impossible to come this far.

TABLE OF CONTENTS

LIST OF FIGURES

CHAPTER I

INTRODUCTION

If a plant has subsections and internal variables can be measured then they can be used for feedback. This kind of control structure is called a cascaded control structure and is useful as it increases the number of degrees of freedom for design. This structure is particularly useful when there is large uncertainty in the plant, considerable sensor noise, nonlinearity etc. In fact in [1] this structure is utilized to stabilize one of the inner loops and then carry out the rest of the design for a class of ballistic type missiles. In [2] QFT is used to design controllers for a three loop cascaded structure for a wind turbine illustrating one of the many applications of cascade design. This thesis analyzes the cascaded loop structure using the tools of QFT developed by Horowitz [3], [4] and H_∞ which originated in the work done in [5].

A. Previous Work

A brief review of the work done in [6] and [7] in designing a cascaded loop control structure using QFT is covered in this section. A linear time-invariant plant having two cascaded sections is considered. The plant transfer functions are $P_1(s)$, $P_2(s)$ and the reference input to the system is r(t) with corresponding Laplace transform R(s). The plant parameters p_i may have considerable uncertainty. The outputs from each of the plants P_1, P_2 can be measured by sensors, the noise characteristics of which are known. The three degrees of freedom of the plants can be used to design the pre-filter F and the controllers G_1(or L_1), G_2(or L_2) in the case of multiple loop design while in the case of single loop design a single controller G is used to meet the specifications. In the multiple loop case feedback from the plant outputs can be allowed only to the initial plant input and not to any of the intermediate plant inputs as this would lead to plant modification. The design objective is to select F, G_1, G_2 or F, G such that :

$$0 \le T_{yr}^{l}(\omega) \le \left|T_{yr}(j\omega)\right| \le T_{yr}^{u}(\omega) \forall\ \omega, \phi_{yr}^{l}(\omega) \le \measuredangle T_{yr}(\omega) \le \phi_{yr}^{u}(\omega)$$
$$, 0 \le T_{ydo}(j\omega) \le T_{ydo}^{u}(\omega) \forall\ \omega, 0 \le T_{ydi}(j\omega) \le T_{ydi}^{u}(\omega) \forall\ \omega, \forall\ P \in \{P\}$$

The journal model is *IEEE Transactions on Automatic Control.*

T_{yr} denotes the closed loop transfer function from the reference to the output with φ_{yr} the corresponding phase. $T_{ydo,}$ T_{ydi} denote the transfer function from disturbance d_o and d_i respectively to the output. The superscripts 1 and u denote the lower and upper limits. The time domain specifications can be converted into frequency domain specifications although there is no rigorous method of doing so. Quite often it is enough to have the magnitude specifications only. This holds good especially for minimum phase plants. For the case of non-minimum phase plants it sometimes becomes necessary to include the phase specifications too.

1. Single Loop Design

The uncertain plants are P_1, P_2. As shown in Fig. 1 (a), the pre-filter F and the controller G are to be designed such that the following specifications are met:

$$0 \le T_{yr}^{l}(\omega) \le \left|T_{yr}(j\omega)\right| \le T_{yr}^{u}(\omega) \,\forall\, \omega \qquad (1)$$

$$0 \le T_{ydo}(j\omega) \le T_{ydo}^{u}(\omega) \,\forall\, \omega \qquad (2)$$

$$0 \le T_{ydi}(j\omega) \le T_{ydi}^{u}(\omega) \,\forall\, \omega, \forall P \in \{P\} \qquad (3)$$

or equivalently $\left|\frac{L}{1+L}\right| \le \mu_1 \quad \forall P \in \{P\}$ (4a)

and $\left|\frac{1}{1+L}\right| \le \mu_2 \quad \forall P \in \{P\}$ (4b)

where L=PG and P=P_1P_2 and {P} is the set of all plants possible.

In essence the objective is to track the reference input at low frequencies and achieve robust stability too. For simplicity it is assumed that P_1, P_2 are minimum phase plants so that the magnitude condition (1) is enough.

The above constraints impose bounds on $L_o(j\omega)$ corresponding to a nominal plant P_o .These bounds are generated by first constructing the plant templates at a set of frequencies spread over the entire frequency range. Corresponding to each frequency a plant template is constructed which is the set of all plants possible at a certain frequency due to uncertainty. The bounds are generated for the nominal loop by sweeping the plant

template for the particular frequency over the Nichols chart to just avoid the M circle corresponding to condition (4a) or N circle corresponding to condition (4b).This is illustrated in Fig. 1(b). The nominal loop L_o=GPo should be outside or on each of these bounds. An optimal design would be such that L_o is on each of the bounds at various frequencies [6], [7] with minimum value of the gain. Loop shaping is done on a Nichols chart. The magnitude of the bounds are high at low frequencies but at high frequencies the bounds form the 'Universal high ω bound (UHωB)'. Since plant templates at high frequencies transform into vertical lines and the plants are of the form $k(j\omega)^{-n}$ where n is the excess of poles over zeros, the size of the UHωB is dependent on the ratio $k_{1max}k_{2max}/k_{1min}k_{2min}$ where k_{1max},k_{2max}, k_{1min} and k_{2min} are the maximum and minimum values of the gain of plants P_1 and P_2.

As mentioned in [6] for minimum phase systems the required specifications can be met with a single loop design but in the case of plants having significant uncertainty the bandwidth of the controller tends to be very high. This can lead to amplification of the sensor noise over a significant frequency range and might result in saturation of the early stages of the plant. This has been the motivation for multiple loop design which is reviewed next.

2. Two Loop Design

Instead of feedback from only the final output we now have the output from the plant P_2 available for feedback as shown in Fig. 2. It is assumed that the inner loop is

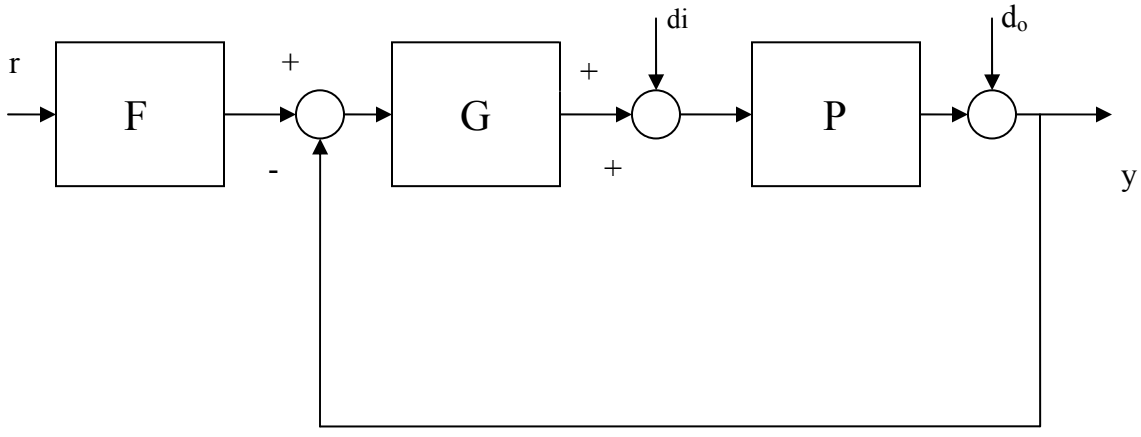

Fig. 1a . Single loop control structure

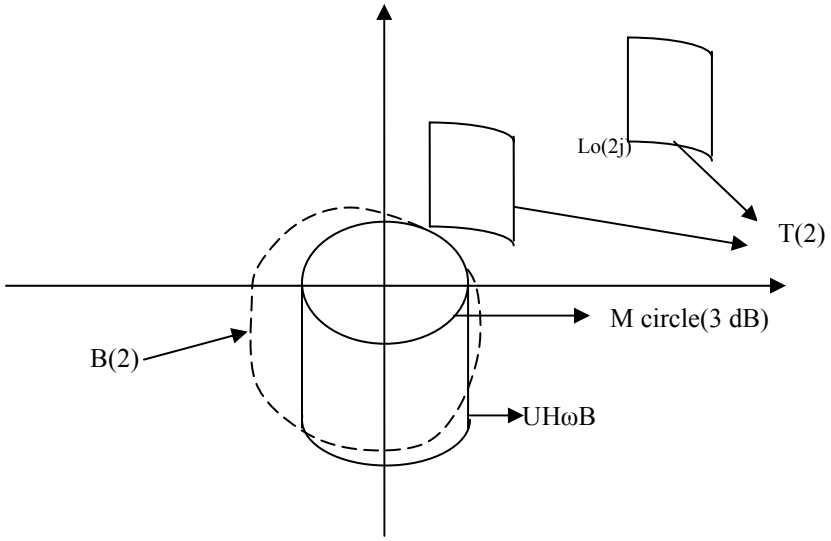

Fig. 1b. Bound generation

T(2)-Template of the plant P(s)=k/(s(s+a)) at 2 rad/s frequency
where k€[1,10],a€ [1,4]
B(2)-Bound for $L_o(2j)$ corresponding to the condition $|L/(1+L)| \leq 3dB \ \forall \ \omega$

almost a perfect one, i.e., the uncertainty in $P_{be}=G_2P_2/(1+G_2P_2)$ is zero and the outer loop L_1 need only handle the uncertainty in P_1. This results in the length of UHωB for nominal loop , L_{10} being only (k_{1max}/k_{1min})dB as at high frequencies any minimum phase plant $P(j\omega)$ transforms to $k(j\omega)^{-n}$ where n is excess poles over zeros. Hence the bandwidth of the controller is much less than the single loop controller decreasing the effects of the outer loop sensor noise considerably.

The inner loop L_2 is then designed such that the uncertainty in P_{be} does not make L_{10} designed above violate it's bounds while preserving stability.

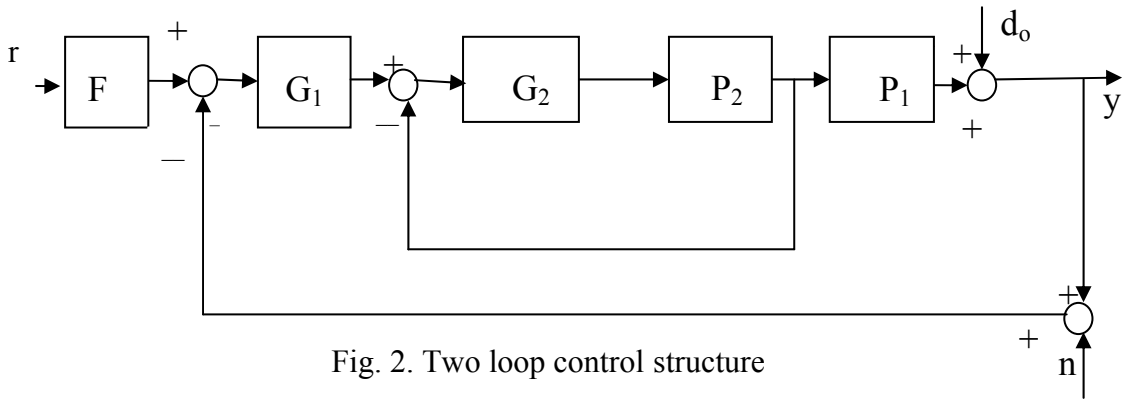

Fig. 2. Two loop control structure

B. Motivation

In a recent paper a two loop controller was designed for the mold level control problem and it was claimed using the simulation results obtained that it has better disturbance rejection characteristics than a single loop design. In this thesis we revisit this issue and make a careful study of the same system from a QFT view point to evaluate and emphasize the merits of two loop designs vs. single loop design. The conditions for existence of a QFT controller is stated in [8]. It is shown using QFT that a single loop design would suffice for specifications in the low frequency for minimum phase systems. Two loops or more design can also be used to meet the same specifications but is not a necessary requirement. This work has been accepted for publication [9].

In the second part of the research the 'outer loop robust stability bounds' for the inner loop of a two loop QFT design are generated analytically using the robust stability condition of the outer loop. This is to be tested only for the higher frequencies where the dominant bounds are the stability bounds. The assumption made while generating these bounds is that at high frequencies the plants templates transform into a line. In [6] a manual way to find these bounds has been described using transparent paper. This method uses the condition that with the design of the inner loop, the outer loop stability bounds are not violated for generating these bounds. This same idea is used for the method proposed in this thesis.

In the third part the inner outer sequential QFT design for cascaded loops is modified .For the two loop case, the inner loop was designed using H_∞ and the outer loop using QFT. The method employed in carrying out this design is very similar to the one used in [10] with the inner loop QFT design being replaced by an H_∞ design. As in [10] the resulting uncertainty after the inner loop is closed is a design specification .This is done by using an appropriate weighting function. Hence the inner loop is to designed to be robustly stable and the sensitivity function is shaped according to the weight used. This can be done easily using H_∞. The controller designed gave very similar results to the ones in [10]. The advantage of this hybrid design is that since the inner loops are to be designed for stability with the sensitivity function to be shaped in a certain way depending on the characteristics of the sensor noise, H_∞ design of the inner loop will add automation to the design apart from the advantages stated in [10]. Also the outer loop being designed using QFT will ensure that the design is not too conservative.

In the fourth part the two loop QFT cascade control design is compared to the H_∞ design. H_∞ designs controllers and pre filters automatically at one go but for this three degree of freedom control structure a number of redundant pre filters and controllers are designed. In total the number of controllers and pre filters designed are nine while the two loop control structure has only three degrees of freedom. Since the same objective using these nine pre filters and controllers can be met using the pre filter and two controllers designed using QFT, the H_∞ design offers no advantage rather it introduces a lot of redundancy and complexity in the design. In [11] the reason for this redundancy is explained and shown with the example of a two degree of freedom system. It is shown that there can be many canonic structures corresponding to a certain number of degrees of freedom with each structure providing no advantage over the other.

C. Organization

The next few sections are organized in the following way. Chapter II compares the design of the single loop controller with two loop controllers. Chapter III covers the computation of ‘robust outer loop stability bounds’ for the inner loop of a two loop design analytically. Chapter IV describes a new method of doing inner-outer loop cascade design with the inner loop being designed using H_∞ and the outer loop using

QFT. Chapter V compares the QFT and H_∞ designs for a two loop cascaded structure. Chapter VI summarizes the conclusions and outlines the future research directions.

CHAPTER II

COMPARATIVE STUDY OF SISO SINGLE LOOP AND MULTIPLE LOOP SYSTEMS

A. Single and Two Loop Design at Low Frequencies

As has been shown in the work done in [6],[7] the inner loop design helps in significant reduction in the uncertainty in P_2.The question then arises whether it is important to have the inner loop for meeting specifications in the low frequencies. It can be shown that the inner loop is not required for this purpose. This is because of the property of free uncertainty explained next.

Now for the two loop design at low frequencies the uncertainty to be handled by $L_1=P_1G_1.(P_2G_2/1+P_2G_2)$ is that of P_1 and $P_{be}=(P_2G_2/1+P_2G_2)$. Let us assume a line template for the plant P_1, $\Gamma(P_1)=20$ dB with the closed loop specification at low frequencies being $\Delta|T_{yr}|\leq 8$ Db. The nominal loop L_0 is designed such that the plant template satisfies the closed loop specification $\Delta|T_{yr}|\leq 8$dB. It can be seen in Fig. 3 that at-130^0 phase angle L_0 should lie between $|T_{min}|$=-5.7 dB and $|T_{max}|$=2.3 dB with the value of L_0 being -7.7 dB. It is very clear from the Fig. that L_0 is satisfactory for uncertainty of the plant much greater than 20 dB .In fact it can handle all the uncertainty in plants P_1 and P_2 without requiring the inner loop to be closed .This is the property of free uncertainty. For some other phase angles of L_0 ,the plant template can even have semi-infinite gain uncertainty.

Design Example:

Let $P=P_1P_2$ be the plant where $P_1=\frac{k_1}{s}, k_1\in[1,10]$ and $P_2=\frac{k_2}{s}, k_2\in[1,20]$

Following are the specifications to be met:

1. Robust Stability $\left|T_{yr}^{l}(\omega)\right|\leq 6\text{dB}\ \forall\omega$
2. Robust Output disturbance rejection:

$$\left|T_{ydo}(j\omega)\right|\leq -30\text{dB}\forall\omega\leq 10 rad/s$$

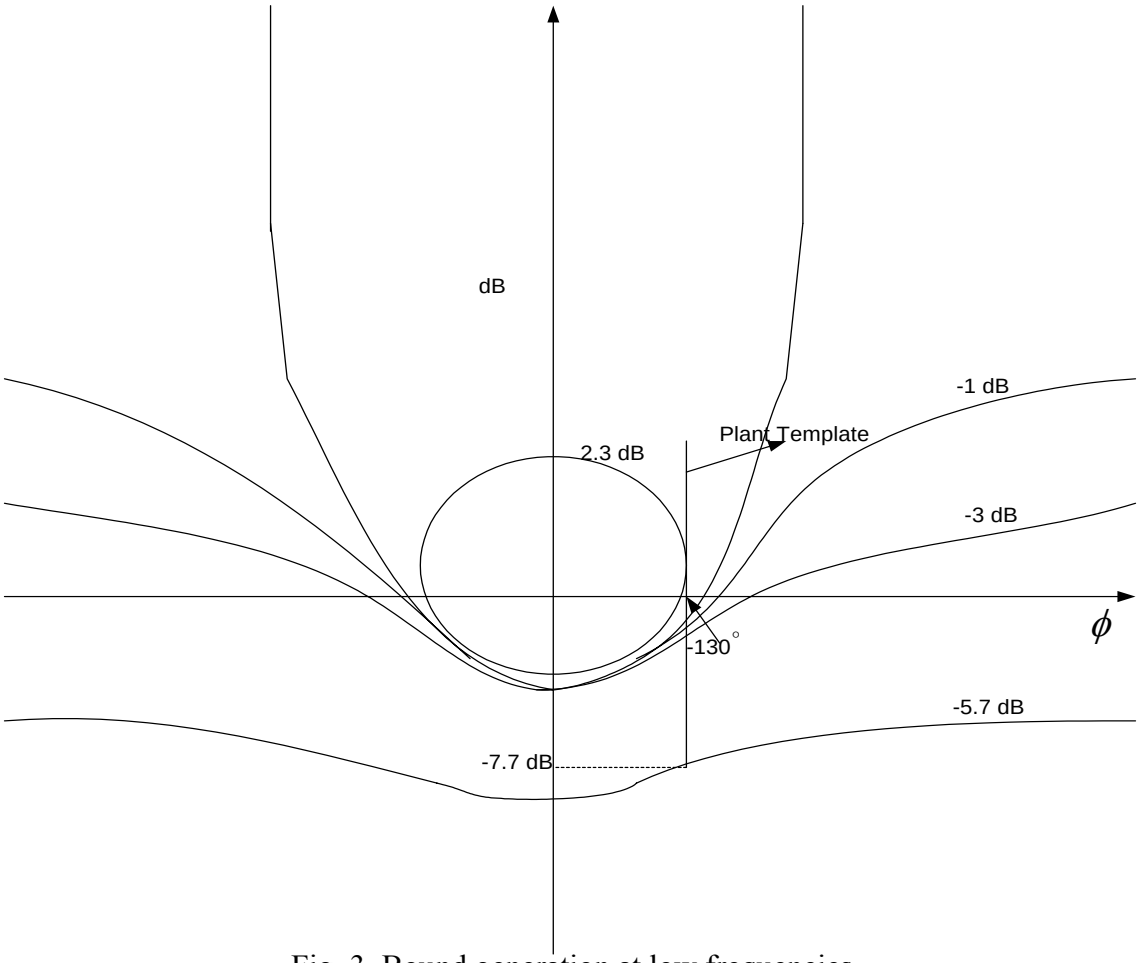

Fig. 3. Bound generation at low frequencies

The nominal loop for the single loop design L_{s0} and the nominal outer loop L_{10} for the two loop design are shown in Fig. 4. Due to the availability of free uncertainty it can very well be seen that the single loop design and the two loop design need not be different upto the frequency ω_a. In the frequency range $[\omega_a, \omega_{x1}]$ the template of P_1 is usually a vertical line and the stability margin constraint dominates over the tracking constraints. Therefore again in this range the bound on L_{10} is the same as that of L_{s0}.

This example again shows that multiple loop design is only necessary when the control objective is in the high frequency range.

Having highlighted the fundamentals of cascaded design we consider the mold level control problem. It is claimed in [12] that a two loop cascade control for mold level has better disturbance rejection properties than a single loop control structure. The theory

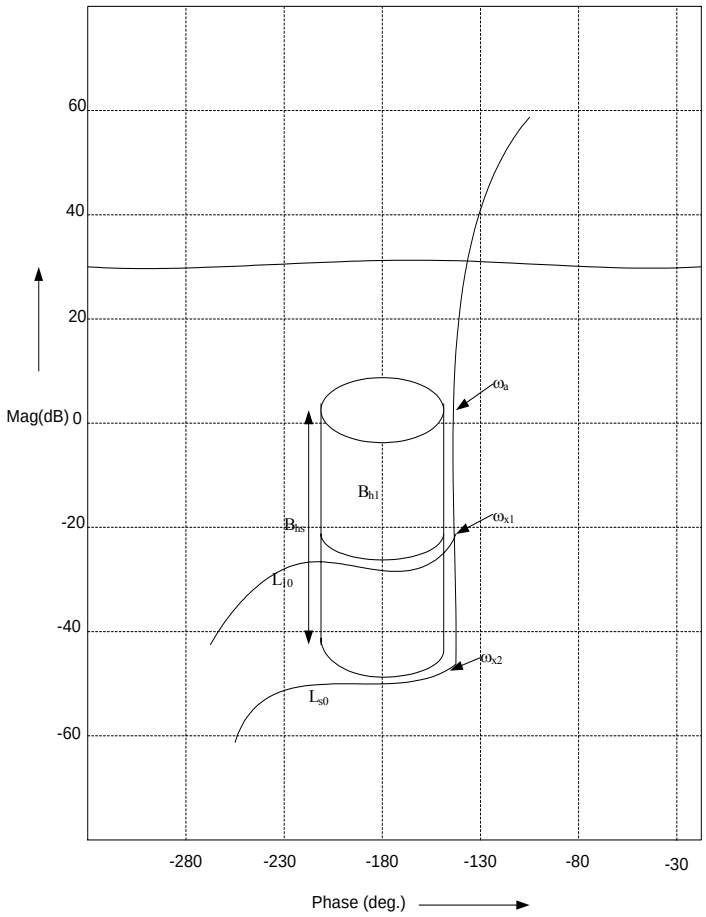

Fig. 4 Loop shaping for single loop and two loop control structure

discussed above is used to show that this is not true with the help of results obtained for the mold level control problem.

B. Mold Level Control Problem

Mold level control is one of the most important factors influencing surface quality of sheets and plates manufactured in a continuous steel casting line. It is a well known fact that accurate mold level control proves to be beneficial. Therefore a lot of research work has been done in this area due to the significant financial stakes involved.

The disturbance in the mold level control processes is periodic. The exact source of this disturbance is not known yet and hence a lot of research has been done to

improve the casting process by better feedback control and better equipment. In [12] this has been attempted with the use of cascade control. The dynamic models for this process has been obtained in [13] with the use of experimental data from an actual casting line. This model has been used to obtain simulation results for this thesis. It has been shown using the above results that cascade control as advocated in [12] is not necessary for meeting the specifications, and that a properly executed single loop design would do.

1. Casting Process Description

Continuous casting is the process of directly solidifying molten steel slabs as they pass through a mold. The process is schematically represented in Fig. 5.

A tundish acts as a reservoir and feeds molten steel to the mold. The stopper valve of the tundish acts as an actuator to control the steel flow into the mold. The hydraulic servo system and stopper rod mechanism are used to achieve this control objective. Depending on the position of the stopper rod molten metal is poured at a specific rate into the mould from the tundish. An eddy current sensor is used to detect the value of the mold level which is compared to the set point to produce a corresponding control signal u.

Cooling of the cast metal occurs in two stages, primary cooling occurring in the mold. This cooling produces a shell around the liquid centre and then this elastic strand is continuously drawn onto supporting rolls where the secondary cooling occurs. The metal is then cut into slabs of appropriate size.

The general assumption is that instabilities in the mold level cause surface defects on the cast metal. Mold level oscillations tend to stir up flux and foreign particles leading to surface defects on the cast metal. These surface defects require to be removed by grinding and this proves to be a big economical loss for steel makers.

The origin of these oscillations is not well known yet. Some of the reasons to which this is attributed to are clogging or wear out of the stopper valve which reduces the effective gain; nonlinearities resulting from the valve geometry and hydraulic whirling of metal flowing into the mold. Another reason is thought to be the periodic changes in the molten metal outflow from the mold due to pressure changes in the elastic strand.

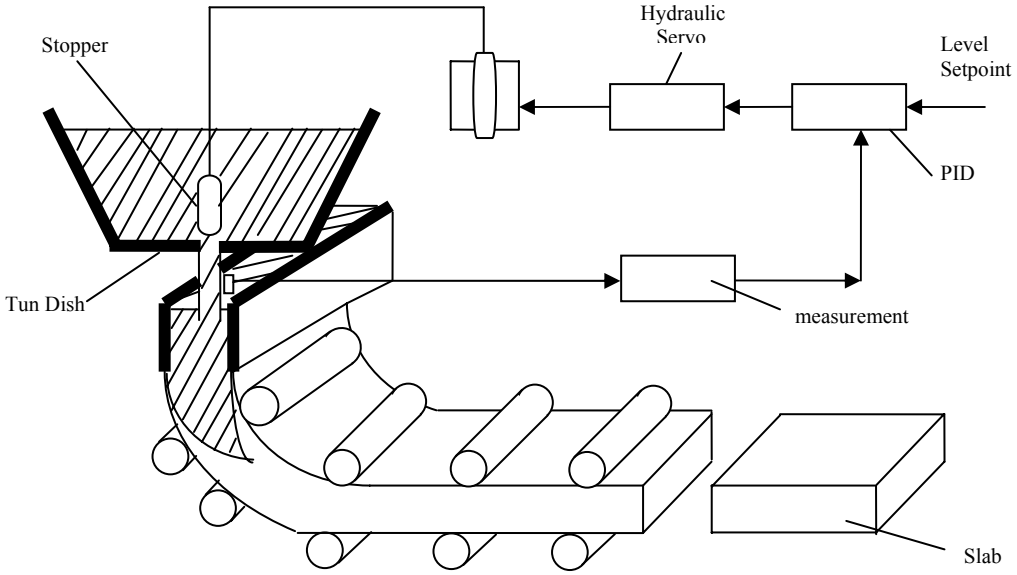

Fig. 5. Casting process

2. Simulation model

The simulation model of the mold process being used is the one developed in [13]. This is illustrated in Fig 6.

Following are the inputs and outputs to the system:

u: control input (stopper position desired in %)

y: controlled output (mold level(mm))

n:(Sensor noise—white noise with s.d. 1mm)

d: out-flow(l/s) which is a disturbance

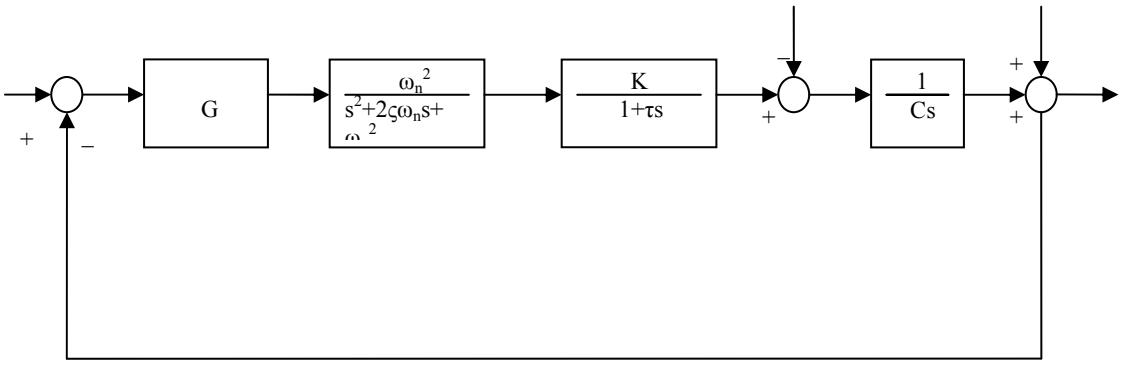

Fig. 6 Simulation model

The outflow d comprises a constant nominal value (10.5 l/s) and a periodic disturbance the power spectral density of which has frequency components in the range of 0.05-0.1 Hz. This is for the case when the amplitude of the disturbances are large.

The hydraulic servo mechanism is modeled by the second order transfer function $\omega_n^2/(s^2+2\zeta\ \omega_n s+\ \omega_n^2)$. The nominal values of the parameters are taken as $\zeta=0.68$ and $\omega_n=6.14$ rad/s [13]. The flow dynamics is represented by the transfer function $K/(1+\tau s)$ the nominal values being $K=1.1$(l/s)/% and $\tau=0.9$s. There is a huge variation in the values of K (gain) of the stopper valve. While designing the controller the value of K was made to vary by 400%. The integrating effect of the mold was modeled by the transfer function 1/Cs where $C=0.42\ m^2$ is the area of the cross section of the mold. A sampling period of 0.001 s was taken for the simulation.

3. Controller Used for Simulation

Quantitative feedback theory was used to design a controller which could meet the objectives of disturbance rejection and also robustly stabilize the plant which has large uncertainty. Bounds were generated on the Nichols chart using the plant templates shown in Fig. 7. It can be very well seen that the plant templates transform into a line at high frequencies. The loop was shaped in a way to be above the low frequency bounds and outside the universal high frequency bounds as shown in Fig. 8. As the disturbance has frequency components in the range of 0.05-0.1 Hz at those frequencies the bound was

generated with the condition $|1/(1+L)| \leq$ -40 dB so that the disturbance has little effect on the output. This condition was obtained from the fact that the transfer function between

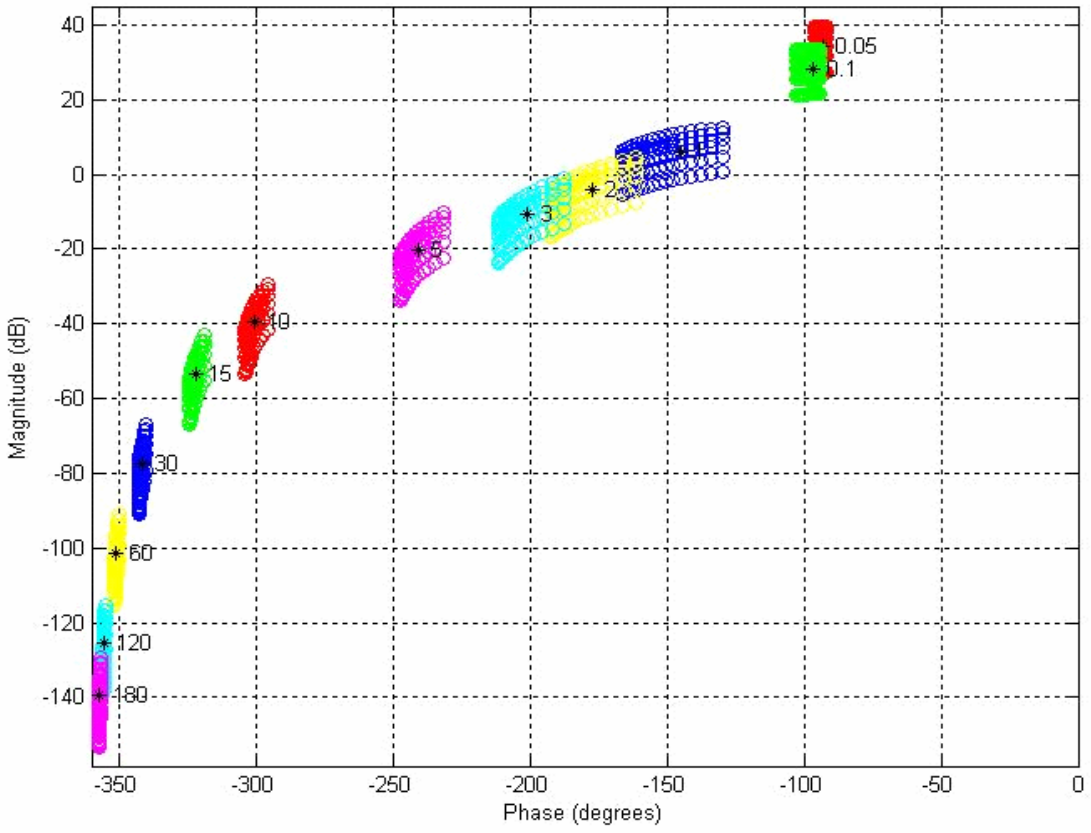

Fig. 7. Plant templates at different frequencies

the output and the output disturbance is 1/(1+L).For robust stability the condition used was $|L/(1+L)| \leq 6$ dB .This condition comes from the fact that for stability the closed should be bounded at the high frequencies. The loop was rolled off at high frequency by adding poles to avoid the adverse effects of high frequency noise. The controller designed was: $\dfrac{3.15(s^2/3.13^2 + 2*0.6*s/3.13 + 1)}{(s^2/105.2^2 + 2*0.15*s/105.2 + 1)*(s^2/69.64^2 + 2*0.24*s/69.64 + 1)}$

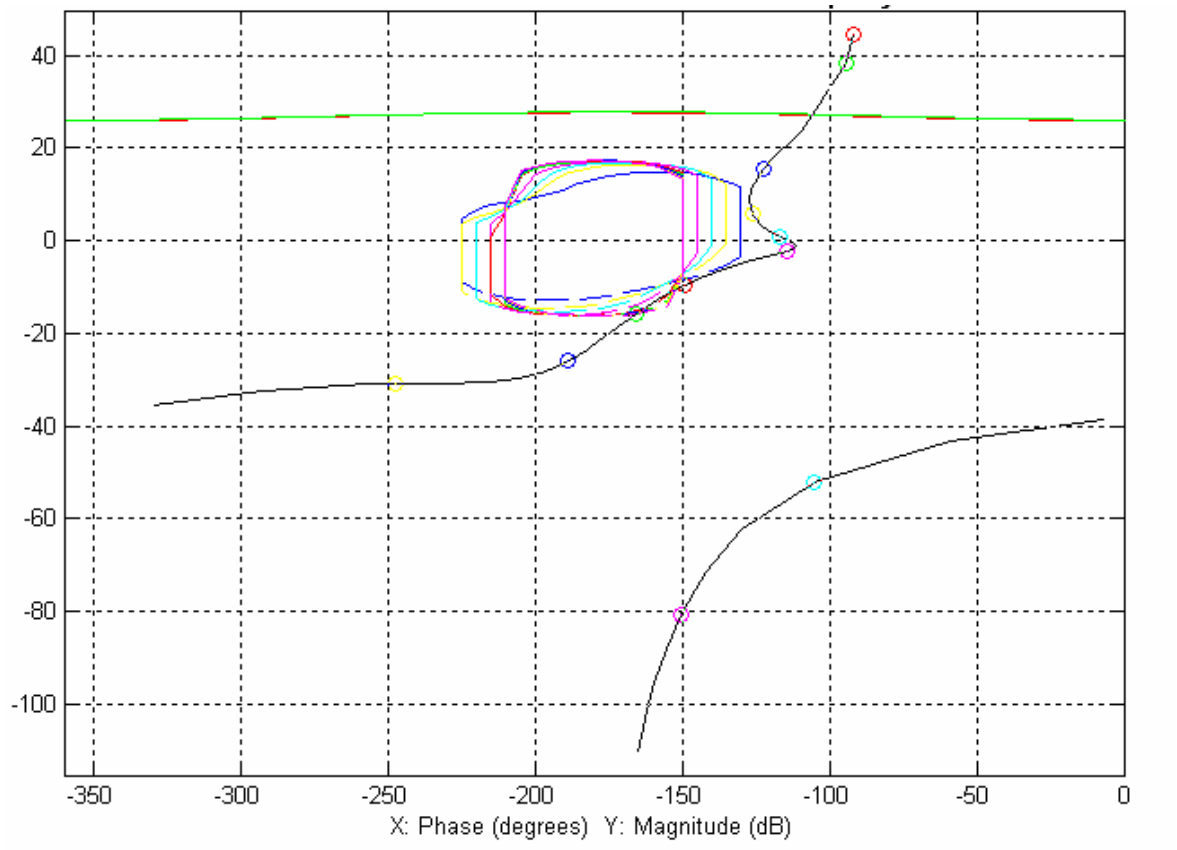

Fig. 8. Loop shaping

C. Performance Comparison with the Two Loop Design

In [12] the results for a two loop master slave control structure is shown and compared to the disturbance rejection characteristics of a single loop controller. It is shown there that the single loop PI controller has poor disturbance rejection characteristics while the two loop control structure gives good results with respect to disturbance rejection.

As can be seen in Fig. 9 our results for a single loop controller compared with the results found in [12] for a two loop design. Apart from the nominal values some other values of k and τ were used to simulate the results. As seen in Fig. 10 the performance is robust with respect to disturbance, the performance being quantified by the standard deviation of the mould level.

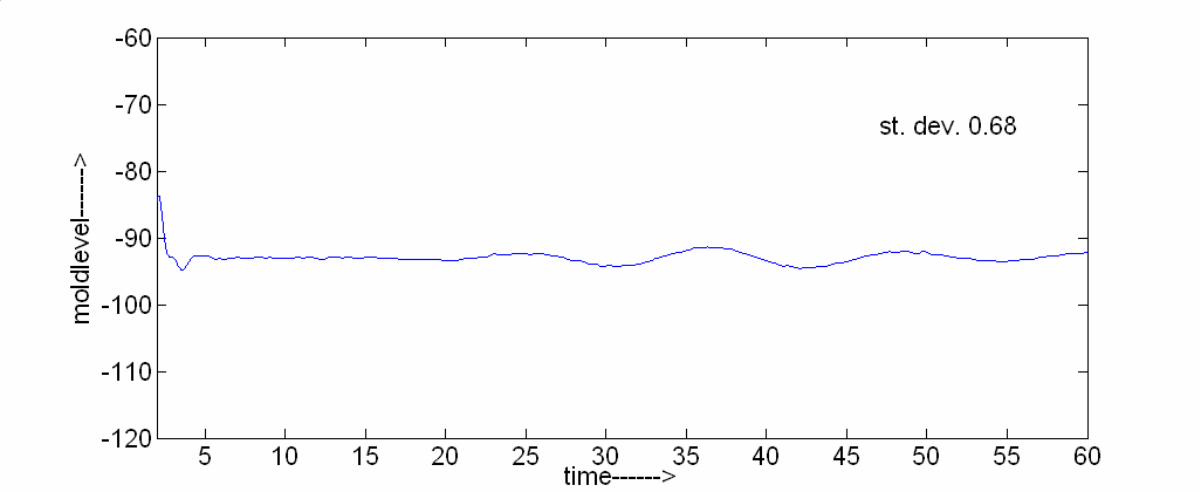

Fig. 9. Simulation result for single loop complex controller for nominal values of plant

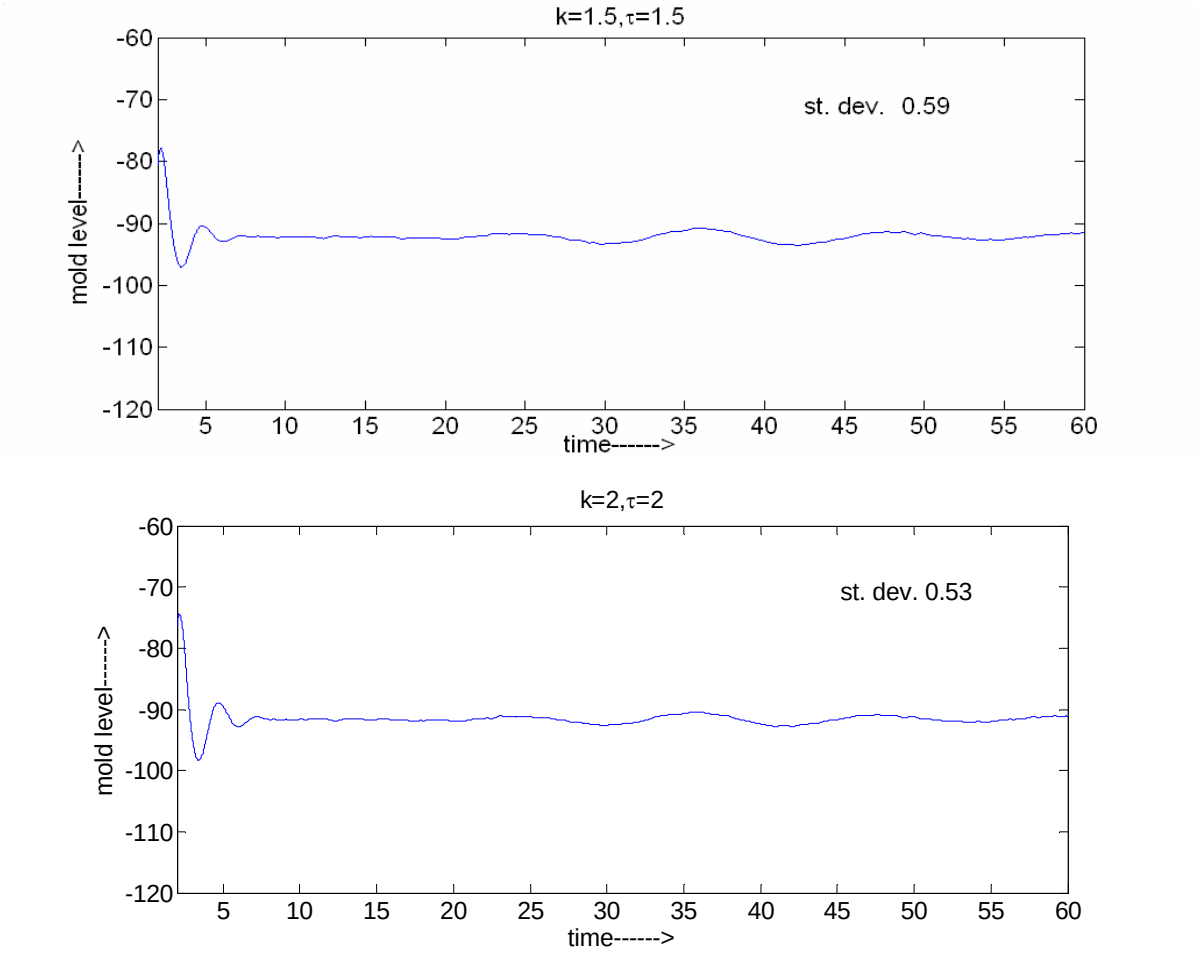

Fig. 10. Simulation result for single loop complex controller for some other values of uncertain parameters

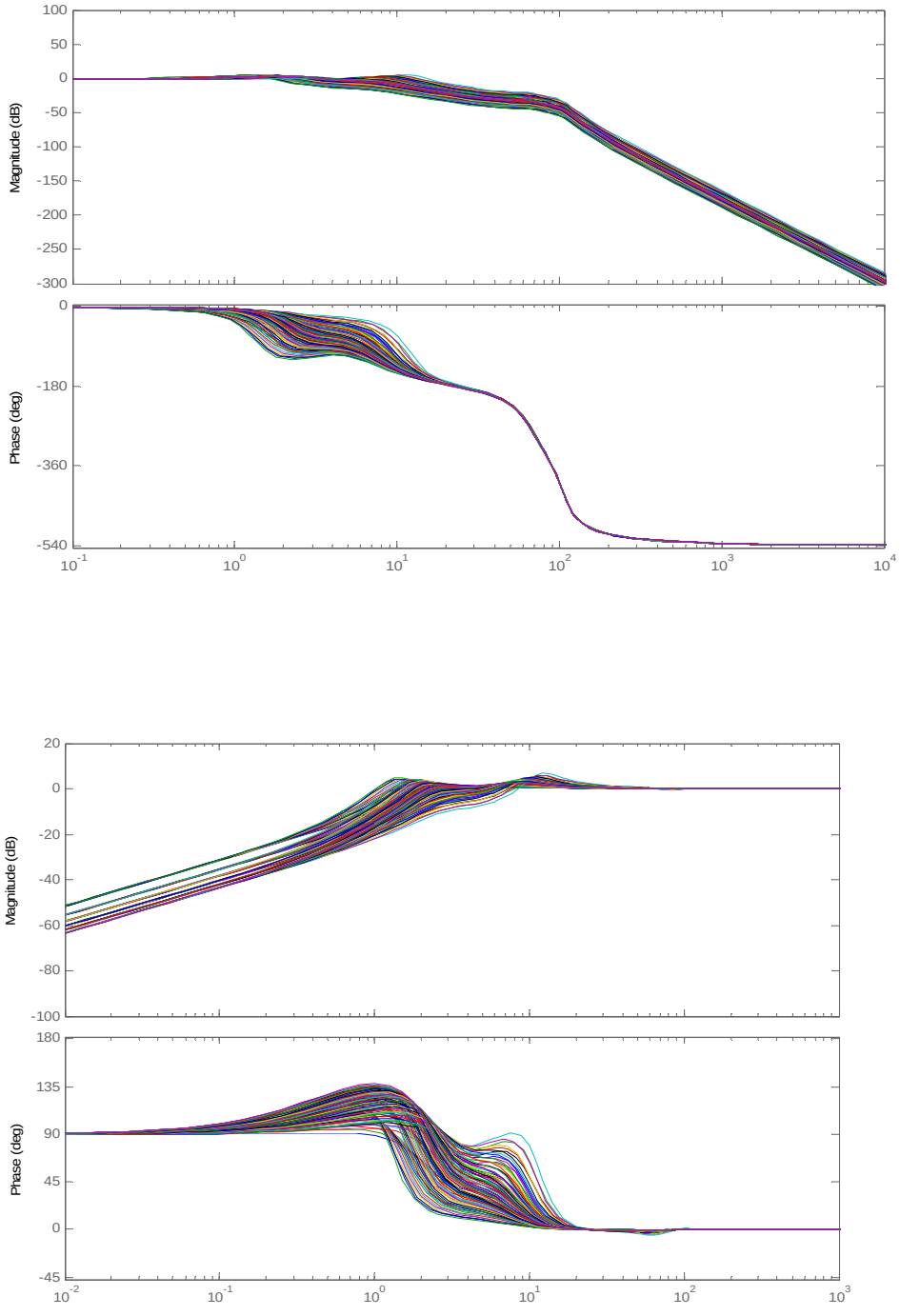

Fig. 11: Closed loop and sensitivity Bode plots

Robust performance is further illustrated in Fig. 11 where the closed loop and sensitivity Bode plots are shown. As far as robustness with respect to process noise is concerned, as in [12] a low-pass filter was used to avoid the ill-effects of noise at the flow process input, i.e., the stopper position thus avoiding mechanical wear of the stopper Therefore it can be said that the control objective is achieved with guaranteed robust stability.

D. Conclusions

In conclusion it can be said that a single loop design could perform as good as a two or more loops design if the specifications are in the low frequency, an example being the disturbance rejection problem. The primary advantage of this is that the design structure is simple and could have an implication on the cost of the design. A disadvantage is that the single loop controller could turn out to be a complex one and noise could be amplified in the case of huge uncertainty of individual plants. In such a situation it would boil down to weighing the advantages and disadvantages and accordingly carrying out the design.

CHAPTER III
ANALYTICAL DESIGN OF ROBUST OUTER LOOP BOUNDS FOR THE INNER LOOP OF A TWO LOOP CONTROL STRUCTURE

A. Inner Loop Bounds in Two Loop Cascade Design

In this section we discuss the two loop cascade design and analytically find the bounds for the inner loop which ensures robust stability of the outer loop. The cascade design can be carried out with closure of the inner loop first and then the outer loop or the outer loop first and then the inner loop. The latter is a more natural approach for closing the loops, the reason being that the inner loop is mainly to reduce the bandwidth of the outer loop controller. If the inner loop were closed first; it may not be evident how much bandwidth is needed for the outer loop to meet the closed loop specifications with minimum bandwidth.

1. Computation of the Bounds for Outer-Inner Design

In the outer-inner design the outer loop is closed first with the assumption that $G_2=\infty$ which means that the uncertainty in the inner loop is zero. The robust stability condition for the outer loop is:

$$\left|\frac{L_1}{1+L_1}(j\omega)\right| \le \mu_1, \forall P_1 \in \mathrm{P}_1, \forall P_2 \in \mathrm{P}_2, \omega \ge 0 \qquad (1)$$

where $L_1 = P_1 G_1 T_2, T_2 = \dfrac{P_2 G_2}{1+P_2 G_2}$

Since $G_2=\infty$, $T_2=1$ which implies $L_1=G_1P_1$ .The nominal loop ($L_{10} = P_{10} G_1 T_{20}, T_{20} = \dfrac{P_{20} G_2}{1+P_{20} G_2}$) is designed to meet all the specifications except for the inner loop margin condition.

Then the inner loop is designed in a manner such that given L_{10} all the specifications are met. The inner loop robust stability condition is given as :

$$\left|\frac{L_2}{1+L_2}(j\omega)\right| \le \mu_2, \forall P_2 \in \mathrm{P}_2, \omega \ge 0 \qquad (2)$$

Again apart from this robust stability condition G_2 is to be designed to maintain robust stability for the outer loop too.

Substituting for L_1 in (1) we get the outer loop margin condition is :

$$\left|\frac{P_1G_1T_2}{1+P_1G_1T_2}(j\omega)\right| \le \mu_1 \qquad (3)$$

Since L_{10} is already designed $G_1 = \frac{L_{10}(1+G_2P_{20})}{P_{10}G_2P_{20}}$ can be substituted in (3). Also substituting the definition of T_2 into (3) yields the following inequality which is the robust stability condition for the outer loop to be maintained while designing the inner loop:

$$\left|\frac{(L_{10}P_1P_2)+(L_{10}P_{20}P_1P_2)G_2}{(P_{10}P_{20}+L_{10}P_1P_2)+(P_{10}P_{20}P_2+L_{10}P_{20}P_1P_2)G_2}\right| \le \mu_1, \forall P_1 \in \mathrm{P}_1, \forall P_2 \in \mathrm{P}_2, \omega \ge 0 \quad (4)$$

Using the above inequality bounds for the inner loop can be generated analytically as given below:

Dividing numerator and denominator of (4) by $L_{10}P_1P_2$ we get

$$\left|\frac{1+P_{20}G_2}{\frac{P_{10}P_{20}}{L_{10}P_1P_2}+1+\left(\frac{P_{10}P_{20}}{L_{10}P_1}+P_{20}\right)G_2}\right| \le \mu_1, \forall P_1 \in \mathrm{P}_1, \forall P_2 \in \mathrm{P}_2, \omega \ge 0$$

Let the inner nominal loop $L_{20}=P_{20}G_2$ be written as $L_{20} = \rho_2(\omega)e^{j\phi_2(\omega)}$. Since these bounds are dominant at frequencies where the P_1 and P_2 templates transform into a line we can safely assume that $\frac{P_1}{P_{10}} = k_1, \frac{P_2}{P_{20}} = k_2$ at the frequencies of interest where k_1 and k_2 are constant gains. Also let us write $L_{10} = \rho_1(\omega)e^{j\phi_1(\omega)}$.Therefore the above inequality transforms to

$$\left|\frac{1+\rho_2(\omega)e^{j\phi_2(\omega)}}{\frac{k_1k_2}{\rho_1(\omega)e^{j\phi_1(\omega)}}+1+\left(\frac{k_1}{\rho_1(\omega)e^{j\phi_1(\omega)}}+1\right)\rho_2(\omega)e^{j\phi_2(\omega)}}\right|\le\mu_1,\forall k_1\in\left[k_{1\min},1\right],$$

$$\forall k_2\in\left[k_{2\min},1\right],\omega\ge 0$$

$$\Rightarrow$$

$$\left|\frac{1+\rho_2e^{j\phi_2}}{\frac{k_1k_2e^{-j\phi_1}}{\rho_1}+1+\frac{k_1\rho_2e^{j\left(\phi_2-\phi_1\right)}}{\rho_1}+\rho_2e^{j\phi_2}}\right|\le\mu_1,\forall k_1\in\left[k_{1\min},1\right],\forall k_2\in\left[k_{2\min},1\right]$$

$$\Rightarrow$$

$$\left|\frac{1+\rho_2\left(\cos\phi_2+j\sin\phi_2\right)}{\frac{k_1k_2\left(\cos\phi_1+j\sin\phi_1\right)}{\rho_1}+1+\frac{k_1\rho_2\left(\cos\left(\phi_2-\phi_1\right)+j\sin\left(\phi_2-\phi_1\right)\right)}{\rho_1}+\rho_2\left(\cos\phi_2+j\sin\phi_2\right)}\right|\le\mu_1,$$

$$\forall k_1\in\left[k_{1\min},1\right],\forall k_2\in\left[k_{2\min},1\right]$$

Since the bound corresponds to equality we can say that the equation below will help in giving us the values of the bound:

$$\left|\left(1+\rho_2\cos\phi_2\right)+j\sin\phi_2\right|=\mu_1\left|\begin{matrix}\left(1+\frac{k_1k_2\cos\phi_1}{\rho_1}+\frac{k_1\rho_2\cos\left(\phi_2-\phi_1\right)}{\rho_1}+\rho_2\cos\phi_2\right)+\\ j\left(\frac{\sin\phi_1}{\rho_1}+\frac{k_1\rho_2\sin\left(\phi_2-\phi_1\right)}{\rho_1}+\rho_2\sin\phi_2\right)\end{matrix}\right|,\Rightarrow$$

$$\forall k_1\in\left[k_{1\min},1\right],\forall k_2\in\left[k_{2\min},1\right]$$

$$\sqrt{\left(1+\rho_2\cos\phi_2\right)^2+\sin^2\phi_2}=\mu_1\sqrt{\begin{pmatrix}\left(1+\dfrac{k_1k_2\cos\phi_1}{\rho_1}+\dfrac{k_1\rho_2\cos\left(\phi_2-\phi_1\right)}{\rho_1}+\rho_2\cos\phi_2\right)^2+\\ \left(\dfrac{\sin\phi_1}{\rho_1}+\dfrac{k_1\rho_2\sin\left(\phi_2-\phi_1\right)}{\rho_1}+\rho_2\sin\phi_2\right)^2\end{pmatrix}},\forall k_1\in\left[k_{1\min},1\right],\forall k_2\in\left[k_{2\min},1\right]$$

If we let $A=\dfrac{k_1k_2}{\rho_1},B=\dfrac{k_1}{\rho_1}$

the above equation becomes:

$$\left(B^2\mu_1^2+2B\mu_1^2\cos\phi_1+\mu_1^2-1\right)\rho_2^2+\begin{pmatrix}2B\mu_1^2\cos\left(\phi_1-\phi_2\right)+2AB\mu_1^2\cos\phi_2+2A\mu_1^2\cos\left(\phi_1+\phi_2\right)+\\ 2\mu_1^2\cos\phi_2-2\cos\phi_2\end{pmatrix}\rho_2$$
$$+\left(\left(2A\cos\phi_1+A^2+1\right)\mu_1^2-1\right)=0$$

Since $\rho_1(\omega),\phi_1(\omega),k_1,k_2$ are all known, ρ_2 can be solved using the above quadratic equation at each ϕ_2

Let us denote

$\left(B^2\mu_1^2+2B\mu_1^2\cos\phi_1+\mu_1^2-1\right)=X$,

$\left(2B\mu_1^2\cos\left(\phi_1-\phi_2\right)+2AB\mu_1^2\cos\phi_2+2A\mu_1^2\cos\left(\phi_1+\phi_2\right)+2\mu_1^2\cos\phi_2-2\cos\phi_2\right)=Y$,

$\left(\left(2A\cos\phi_1+A^2+1\right)\mu_1^2-1\right)=Z$

Then the above equation becomes:

$X\rho_2^2+Y\rho_2+Z=0$

and

$$\rho_2=\frac{-Y\pm\sqrt{Y^2-4XZ}}{2X}$$

Since

$\rho_2=\dfrac{-Y-\sqrt{Y^2-4XZ}}{2X}$ is not permissible as ρ_2 is a positive quantity,

$$\rho_2=\frac{-Y+\sqrt{Y^2-4XZ}}{2X}$$

The bound at a particular frequency can be found out by first finding the value of ρ_1 and ϕ_1 using the already known L_{10} and using it to calculate the maximum ρ_2 at each phase angle when k_1 and k_2 are varied between [k_{1min},1and [k2min,1] respectively.
The outer-inner example in [14] was used to illustrate the method as shown below:

2. Design Example

The plants $P_1(s)$ and $P_2(s)$ have parametric uncertainty and are given as follows:

$$P_1(s) = \frac{1}{(s+a)(s+b)}, a \in [1,5], b \in [20,30],$$
$$P_2(s) = k, k \in [1,10]$$

The performance specifications are :

1. Robust margins: 50 degree phase margin in each loop;

2. Robust output disturbance rejection

$$\left|\frac{Y(j\omega)}{D(j\omega)}\right| < 0.02\left|\frac{(j\omega)^3 + 64(j\omega)^2 + 748(j\omega) + 24}{(j\omega)^2 + 14.4(j\omega) + 169}\right|, \omega < 10;$$

3. Robust inner disturbance rejection

$$\left|\frac{Y(j\omega)}{V(j\omega)}\right| < 0.01, \omega < 50.$$

The outer loop margin bounds for the inner loop were generated using the method stated for two frequencies, $\omega = 25 rad/s, 50 rad/s$ as shown in Figs. 12 and 13.

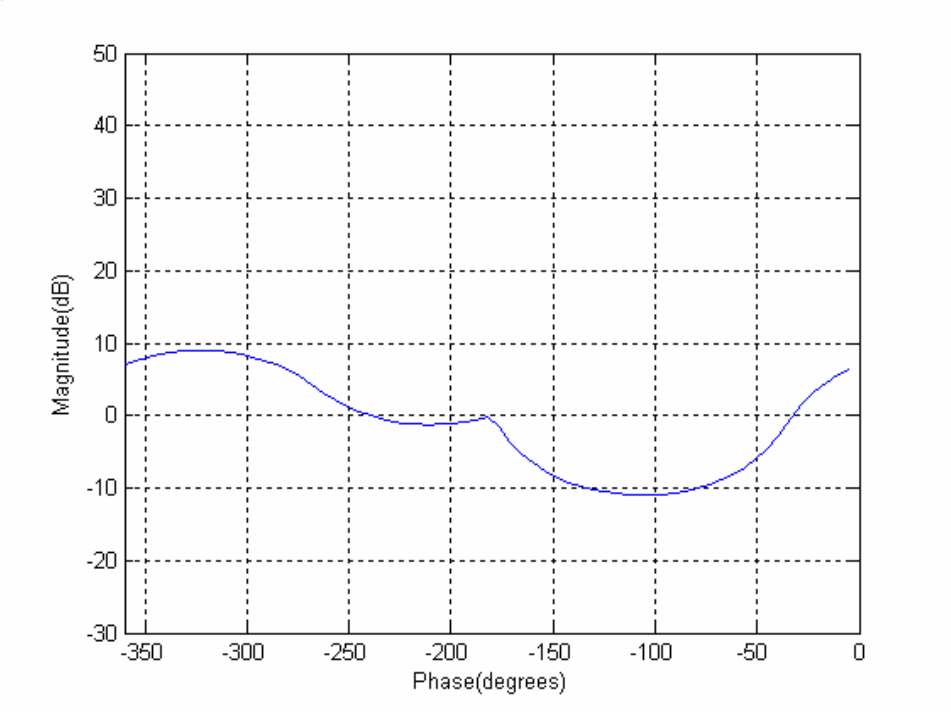

Fig. 12. Bound at $\omega = 25 rad/s$

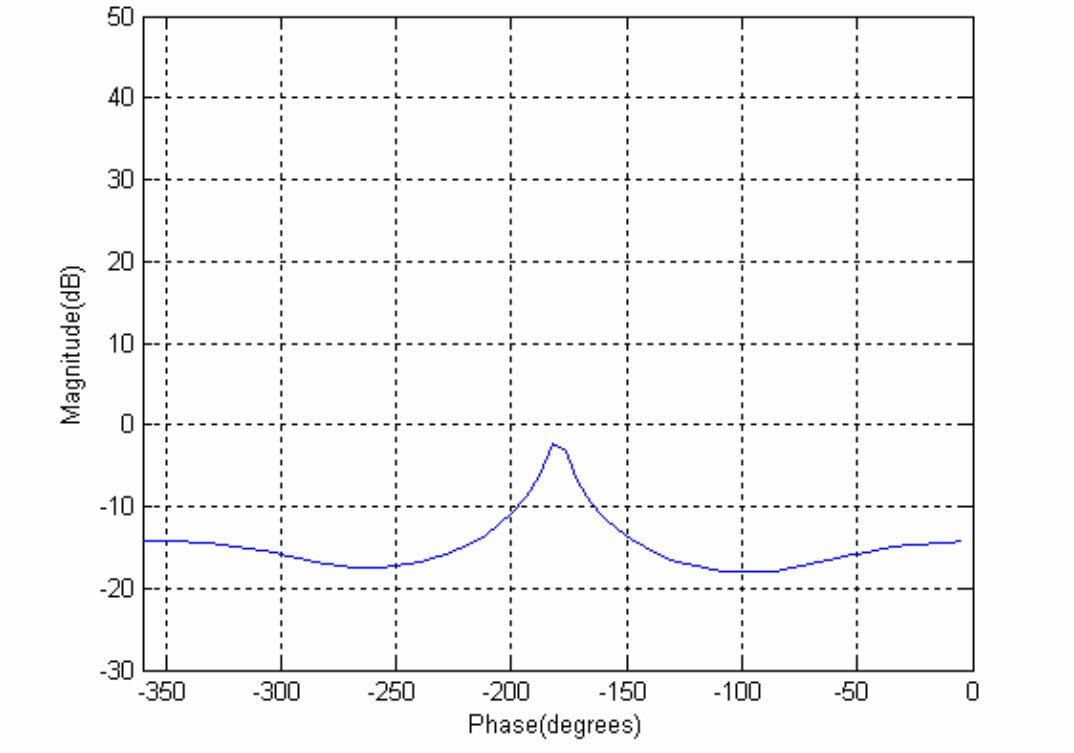

Fig. 13 Bound at $\omega = 50 rad/s$

B. Conclusion

From the design example worked out it can be seen that the analytical way can be alternately used to compute the outer loop robust stability bounds for the inner loops. The inequations found could be used for finding the property of these bounds .These properties could be like the phase angle at which the bounds have maximum magnitude.

CHAPTER IV
HYBRID DESIGN OF CASCADED SYSTEMS USING QFT AND H_∞

A. Inner-Outer Cascade Design Using QFT AND H_∞

In [10] a new method has been proposed for the design of SISO Cascaded-Loop. This method is different from the conventional inner-outer and outer-inner design procedures. The uncertainty which results in the inner loop is made a design specification by introducing a weight function. This weight determines the control burden allocation between the inner and outer loop controllers. In fact this allocation depends on the sensor noise spectra of each loop. Therefore the inner loop design becomes a sensitivity reduction problem whereas the outer loop design involves a plant with mixed uncertainty and it's design is carried out in the usual way. In [10] both the inner loop and the outer loop designs are carried out using Quantitative Feedback Theory. Since the inner loop design is to be carried out for sensitivity reduction and robust stability it can be done using H_∞. The algorithm used for the H_∞ design has been stated in [15]. This would help in automating the design. The outer loop design is then carried out in the usual way using QFT.

1. Design Method

Since the overall loop transfer function for the cascaded control structure shown in Fig. 14 is $L_1=G_1T_2P_1=L_{10}P_1T_2/P_{10}T_{20}$ where $L_{10}=G_1P_{10}T_{20}$, uncertainty is there in P_1T_2 unlike assumption of uncertainty only in P_1 in the outer-inner design procedure while designing the outer loop. Therefore the plant while designing G_1 is P_1T_2 which can be written as

$P_1T_2=P_1T_{20}(1+ (T_2- T_{20})/ T_{20})$

The uncertainty in T_2 may be bounded by $l(\omega)$ at each frequency which implies :

$$\left|\frac{T_2 - T_{20}}{T_{20}}\right| \le l(\omega), \forall P_2 \in \{P_2\} \qquad (1)$$

Hence the actual problem is embedded in the mixed uncertainty problem with equivalent plant:

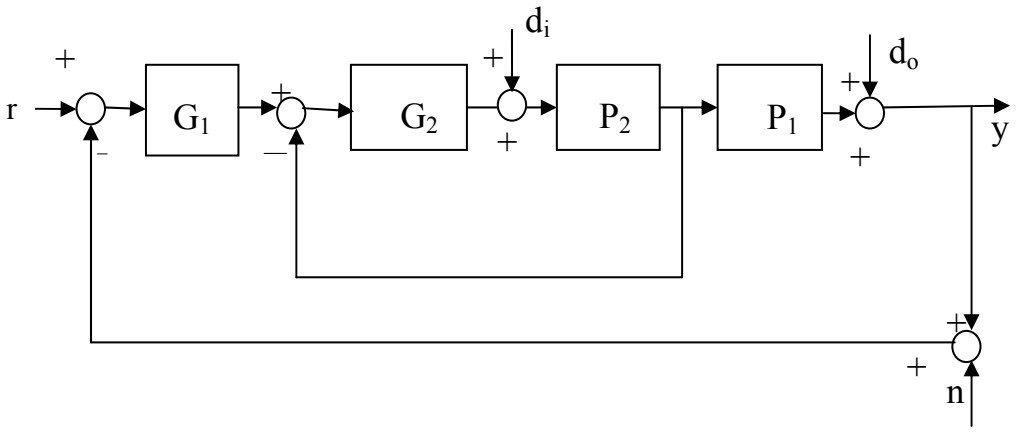

Fig. 14. Cascaded control structure

$$P_{12} = P_1 T_{20}\left(1+\Delta\right), \forall P_1 T_{20} \in \left\{P_1 T_{20}\right\}, \forall \left|\Delta\right| \le l\left(\omega\right), \Delta \in H_\infty$$

The standard QFT method can be then used to design L_{10}. It is to be noted that since a larger class of uncertainty is being handled, conservatism creeps in at this stage.

To set up the bound $l\left(\omega\right)$ the nominal plant P_{20} is chosen to be at or near the center of the uncertainty set $P_{20}\left(j\omega\right)$ which can be done by observing the plant templates on the complex plane at certain frequencies. $l_{\min}\left(\omega\right)$ is then selected such that:

$$\left|P_2 - P_{20}\right| \le l_{\min}\left(\omega\right), \forall P_2 \in \left\{P_2\right\} \qquad (2)$$

or equivalently

$$P_2 = P_{20} + \Delta_2 l_{\min}, \left\|\Delta_2\right\|_\infty \le 1$$

where $l_{\min}\left(\omega\right)$ is the smallest radius at each frequency which covers the entire structured uncertainty set. This way of defining the entire plant set has been used in [7] for interval plants.

Again,

$$\left|\frac{T_2 - T_{20}}{T_{20}}\right| = \left|\frac{1}{1+G_2P_2}\right|\left|\frac{P_2 - P_{20}}{P_{20}}\right| \tag{3}$$

using (4) we get

$$\left|\frac{T_2 - T_{20}}{T_{20}}\right| \le \frac{|S_2| l_{\min}(\omega)}{|P_{20}|} \tag{4}$$

where S_2 is the inner loop sensitivity function. Now, depending on the sensor noise spectra and other design specifications a weight is introduced such that

$$|S_2| \le W_2(\omega), \forall P_2 \in \{P_2\} \tag{5}$$

which is equivalent to

$$\|S_2\|_\infty \le W_2(\omega), \forall P_2 \in \{P_2\} \tag{6}$$

Let $l(\omega) = \dfrac{W_2(\omega) l_{\min}(j\omega)}{|P_{20}|}$ (7)

Using equations (4),(5) and (6) we get

$$\left|\frac{T_2 - T_{20}}{T_{20}}\right| \le l(\omega) \tag{8}$$

As stated in [10],with the use of the weight function the design of G_1 and G_2 are effectively decoupled. $W_2(\omega)$ determines the control burden of G_1 and G_2,their bandwidth and the amount of uncertainty in the inner loop. Since the inner loop is to be designed using H_∞ the standard H_∞ sensitivity reduction problem is used to determine the weight. The technique used in [16] can be used to set up the weight as

$$W_2 = \frac{s + \omega_B A}{s/M + \omega_B}, A \le (or \ll) 1, M \ge 1 \tag{9}$$

where A is the upper bound for the weight at low frequencies, M is the upper bound at high frequencies and ω_B is the sensitivity bandwidth(approximately).

Therefore the inner loop H infinity problem reduces to :

$$\left\| \frac{1}{(1+G_2P_2)W_2(\omega)} \right\|_\infty \le 1, \forall P_2 \in \{P_2\},\ \text{(Robust Performance condition)}$$

$$\left\| \frac{G_2 l_{\min}}{1+G_2P_{20}} \right\|_\infty \le 1 \text{ (Robust Stability condition)}$$

Let us denote W_y=1/W$_2$

The LFT formulation of the inner loop is given in Fig. 15.

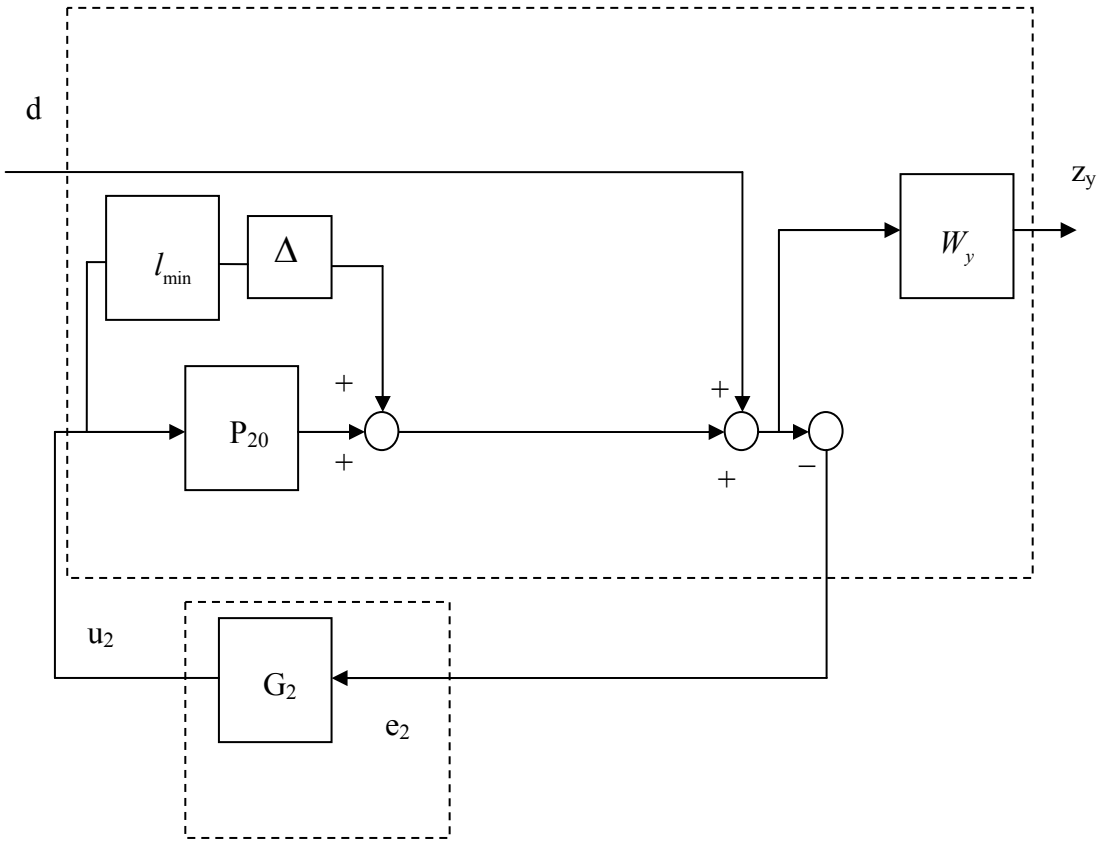

Fig. 15. LFT formulation for the inner loop

To solve the above H_∞ problem using the software tools available the above LFT formulation is modified using the method used in [17] as shown in Fig. 16.

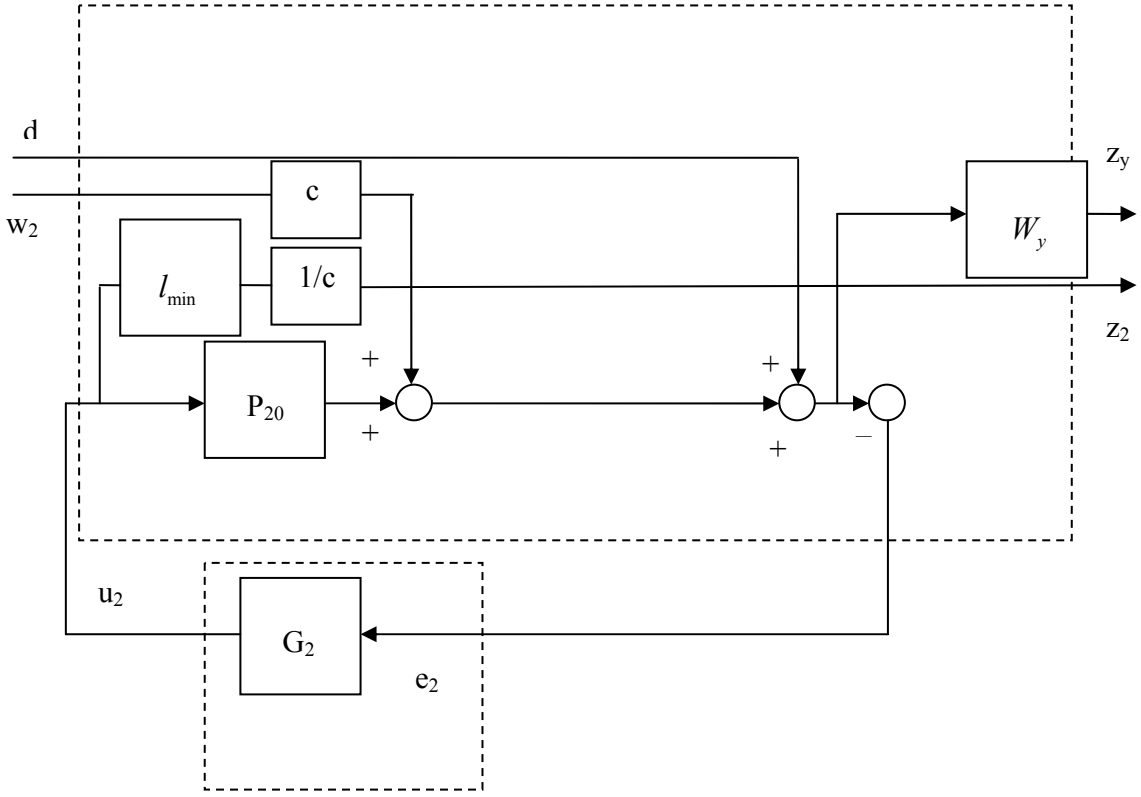

Fig. 16. Modified LFT formulation of the inner loop

In Fig. 16

$$z = \begin{bmatrix} z_2 \\ z_y \end{bmatrix} \qquad w = \begin{bmatrix} d \\ w_2 \end{bmatrix}$$

$$y = \begin{bmatrix} e_2 \end{bmatrix} \qquad u = \begin{bmatrix} u_2 \end{bmatrix}$$

where z, y, w and u are the error variables, measured variables, exogenous inputs and control inputs to the system respectively.

$$P_{zw} = \begin{bmatrix} 0 & 0 \\ W_y & cW_y \end{bmatrix}$$

$$P_{zu} = \begin{bmatrix} \frac{l_{\min}}{c} \\ P_{20}W_y \end{bmatrix}$$

$$P_{yw} = \begin{bmatrix} -1 & -c \end{bmatrix}$$

$$P_{yu} = \begin{bmatrix} -P_{20} \end{bmatrix}$$

where P_{zw} ,$P_{zu,}$ P_{yw},P_{yu} are the open loop transfer functions from z to w, z to u, y to w and y to u respectively.

$$N_{zw} = P_{zw} + P_{zu}K\left(I - P_{yu}K\right)^{-1} P_{yw}$$

where N_{zw} is the closed loop transfer function from z to w.

Using the open loop transfer functions given above

$$N_{zw} = \begin{bmatrix} -\frac{l_{\min}G_2}{c\left(1+P_{20}G_2\right)} & -\frac{l_{\min}G_2}{\left(1+P_{20}G_2\right)} \\ \frac{W_y}{1+P_{20}G_2} & \frac{cW_y}{1+P_{20}G_2} \end{bmatrix}$$

Since the H infinity methodology minimizes the infinity norm of N_{zw} it can be seen that the if $\left\|N_{zw}\right\|_\infty \le 1$ condition is met then robust stability and nominal performance will be achieved. For robust performance c can be varied till $\left\|\frac{W_y}{\left(1+G_2P_2\right)}\right\|_\infty \le 1, \forall P_2 \in \left\{P_2\right\}$,

is satisfied.

2. Design Example

The example problem solved in [10] , [14] is redone here.

The above approach is used to solve this problem.

The plants $P_1(s)$ and $P_2(s)$ have parametric uncertainty and are given as follows:

$$P_1(s) = \frac{1}{(s+a)(s+b)}, a \in [1,5], b \in [20,30],$$
$$P_2(s) = k, k \in [1,10]$$

The performance specifications are :

1. Robust margins: 50 degree phase margin in each loop;

2. Robust output disturbance rejection

$$\left|\frac{Y(j\omega)}{D(j\omega)}\right| < 0.02\left|\frac{(j\omega)^3 + 64(j\omega)^2 + 748(j\omega) + 24}{(j\omega)^2 + 14.4(j\omega) + 169}\right|, \omega < 10;$$

3. Robust inner disturbance rejection

$$\left|\frac{Y(j\omega)}{V(j\omega)}\right| < 0.01, \omega < 50.$$

Since $P_2(s)=k, k\varepsilon[1,10]$, $P_{20}=5.5$ is taken at the centre of the plant template at all frequencies. This means $l_{min}=10-5.5=4.5$

As in [12] the sensitivity function is taken as

$$W_2 = \frac{s + \omega_B A}{s/M + \omega_B}, A = 0.01(-40dB), M = 1.2, \omega_B = 2 \times 10^4$$

$G_2(s)$ is then designed for robust stability and nominal performance. To achieve robust performance c was varied till $\left\| \frac{W_y}{(1+G_2P_2)} \right\|_\infty \leq 1, \forall P_2 \in \{P_2\}$ was satisfied.

Once G_2 was designed ,G_1 was designed for the specifications (6),(7) and (12) using the standard QFT method. MATLAB QFT Toolbox [14] was used to do this. The nominal plant used was $T_{20}P_{20}$ to design the loop $L_{10}= G_1T_{20}P_{20}$.

Since H_∞ gave a controller with e=0,the degree difference between the numerator and denominator, poles were added at high frequency for roll off to the H infinity design.

The controllers designed were:

$$G_2 = \frac{113.4\left(s/2.088\times10^6+1\right)}{\left(s/200+1\right)\left(s/7\times10^5+1\right)^2}$$

$$G_1 = \frac{392.9}{\left(s/152.8+1\right)\left(s^2/509.1^2+2\times0.2377s/509.1+1\right)}$$

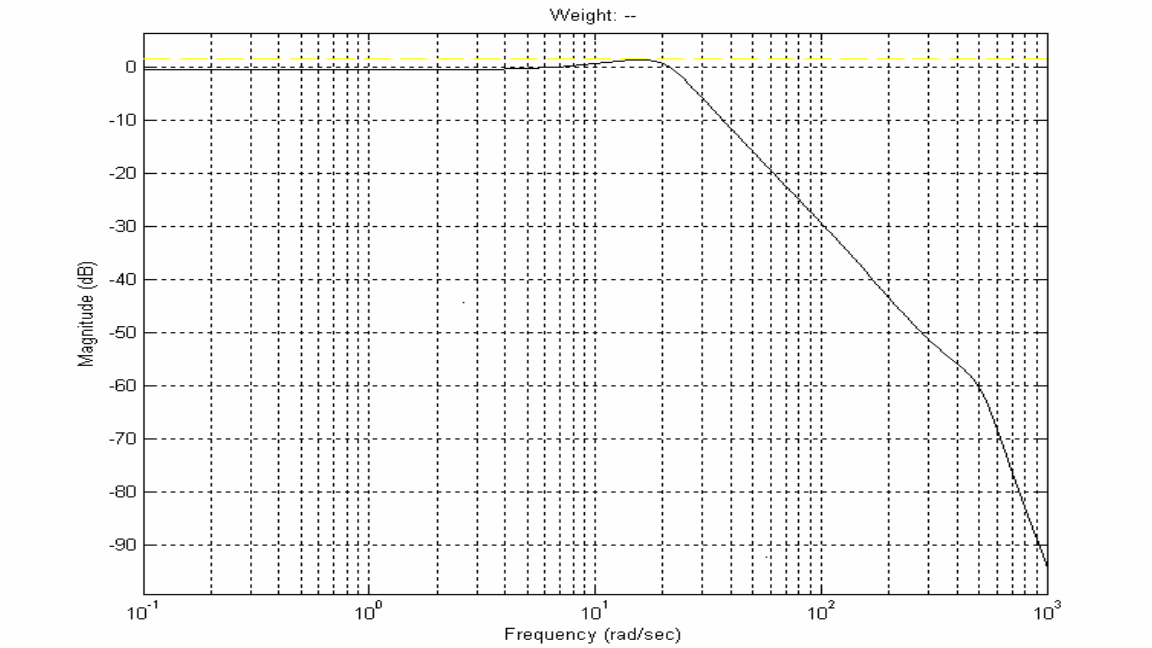

Fig. 17: Robust margin specification

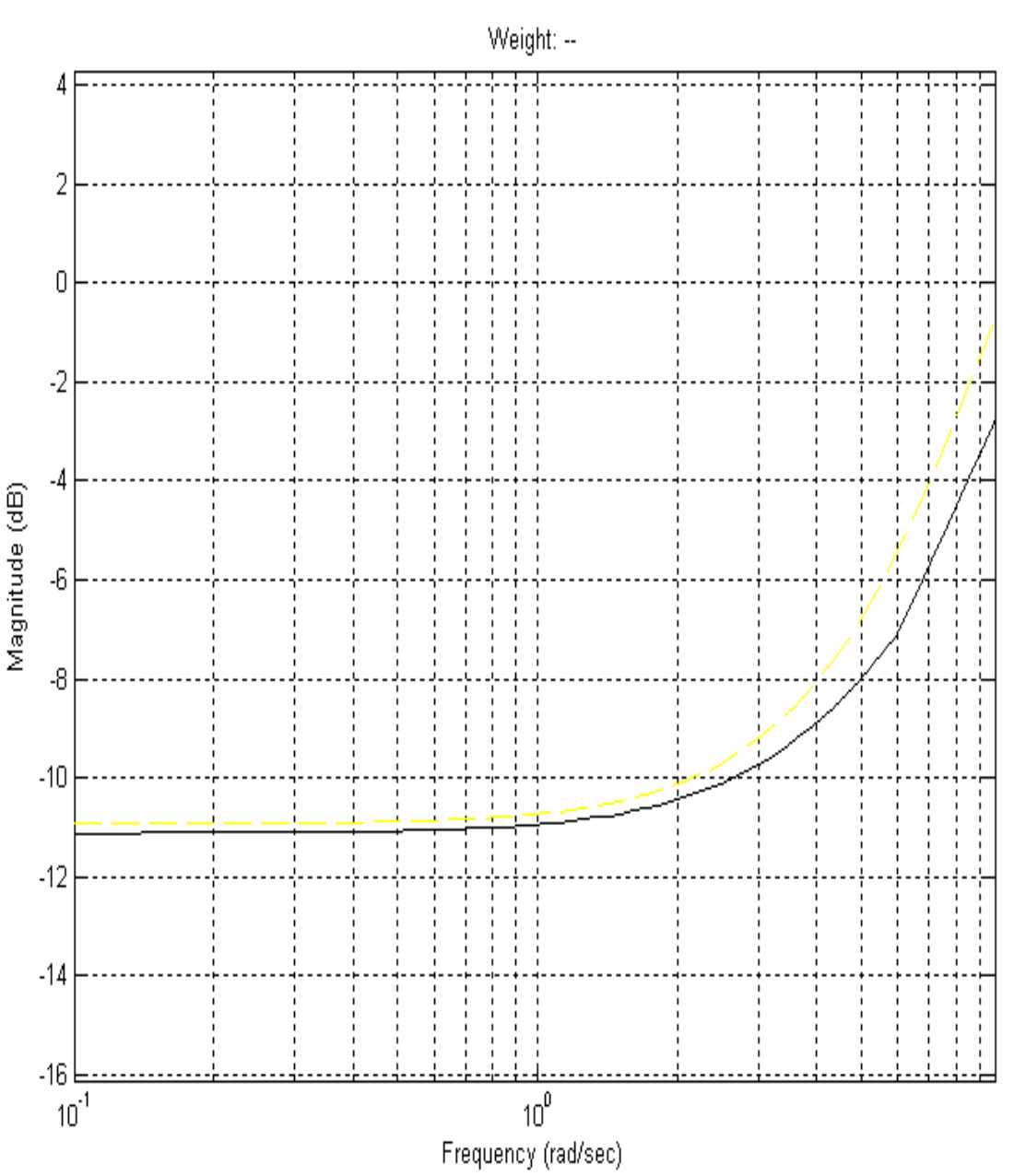

Fig. 18: Output disturbance rejection specification

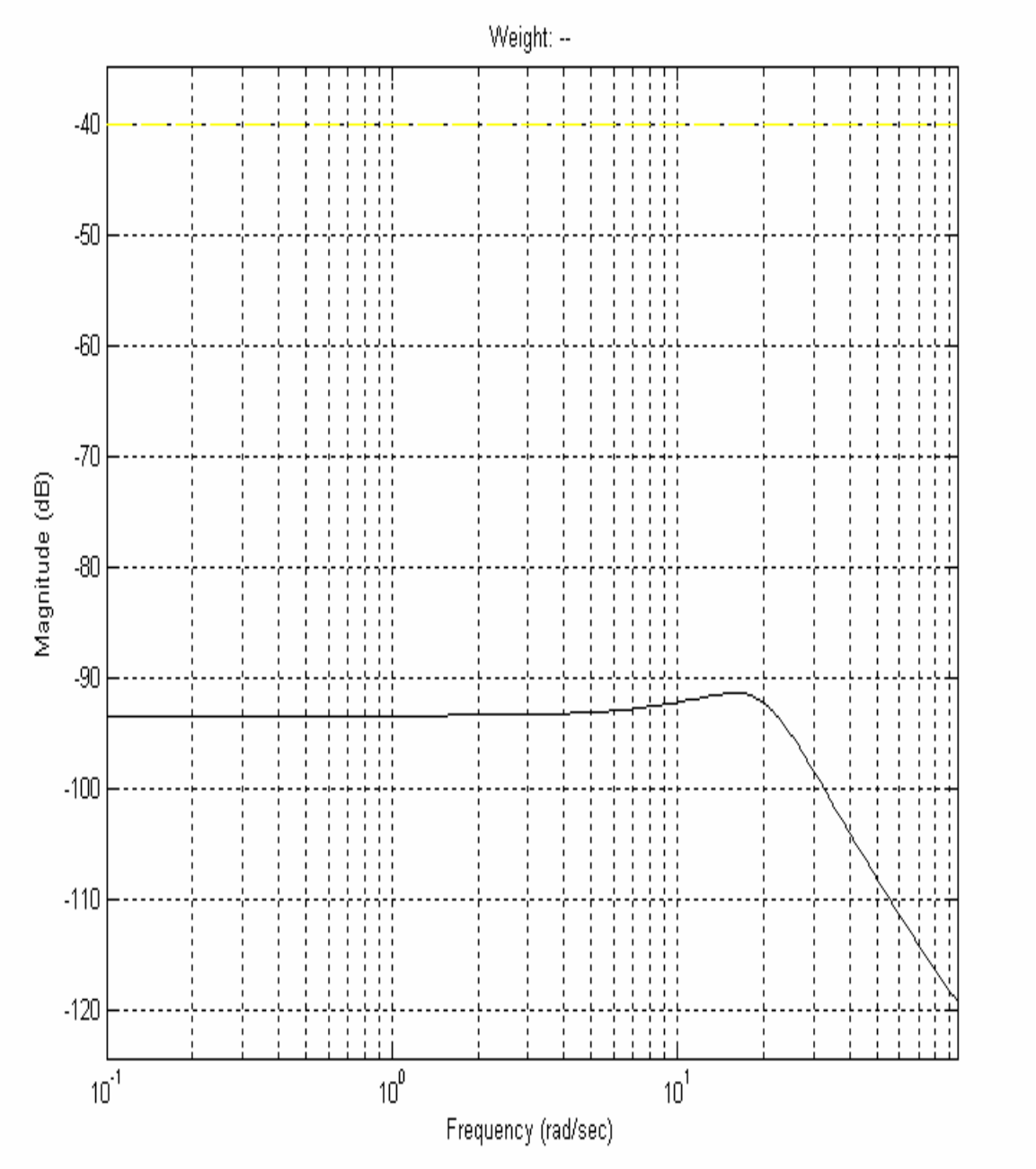

Fig. 19: Robust input disturbance rejection

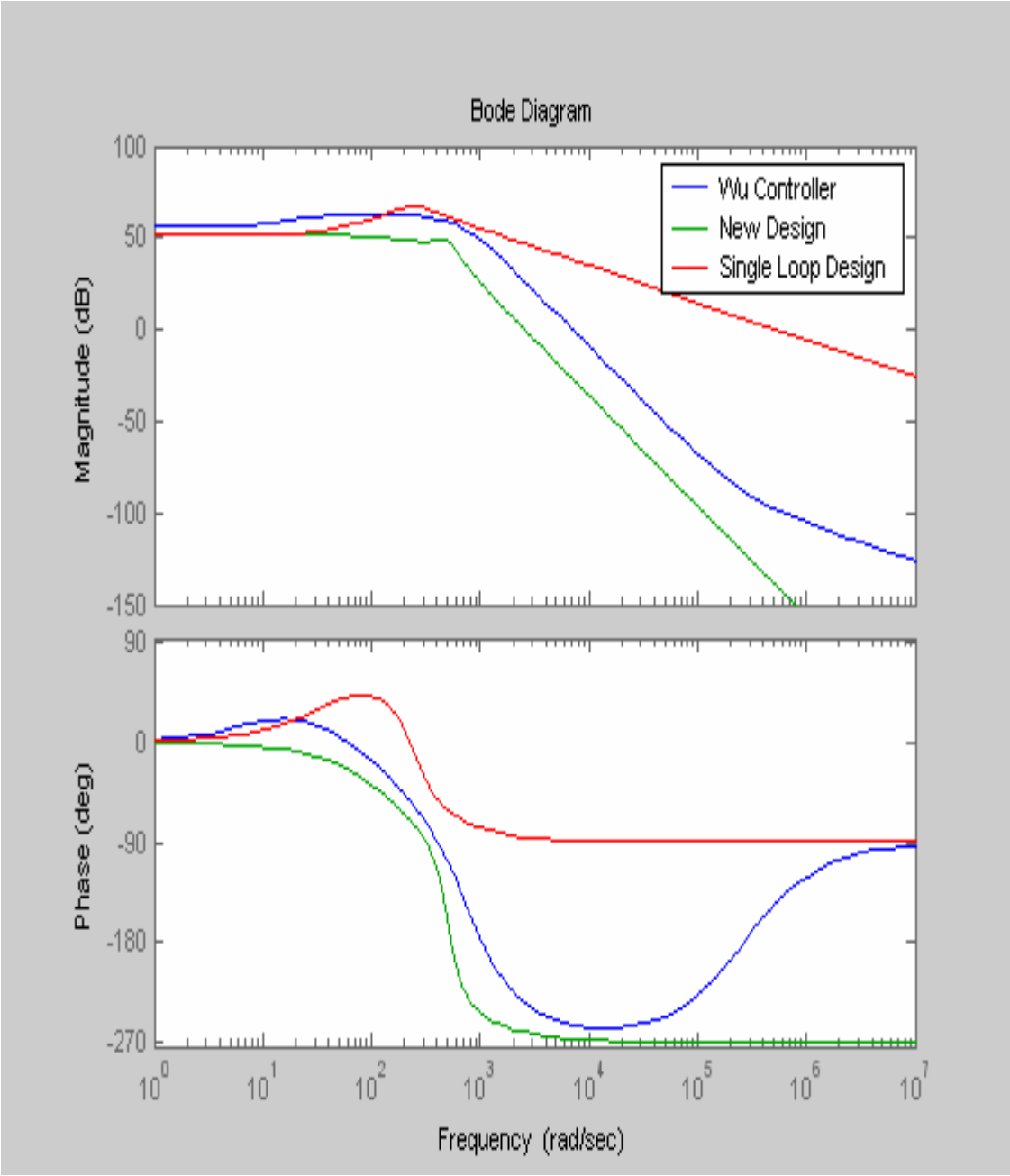

Fig. 20: Outer loop controller comparison

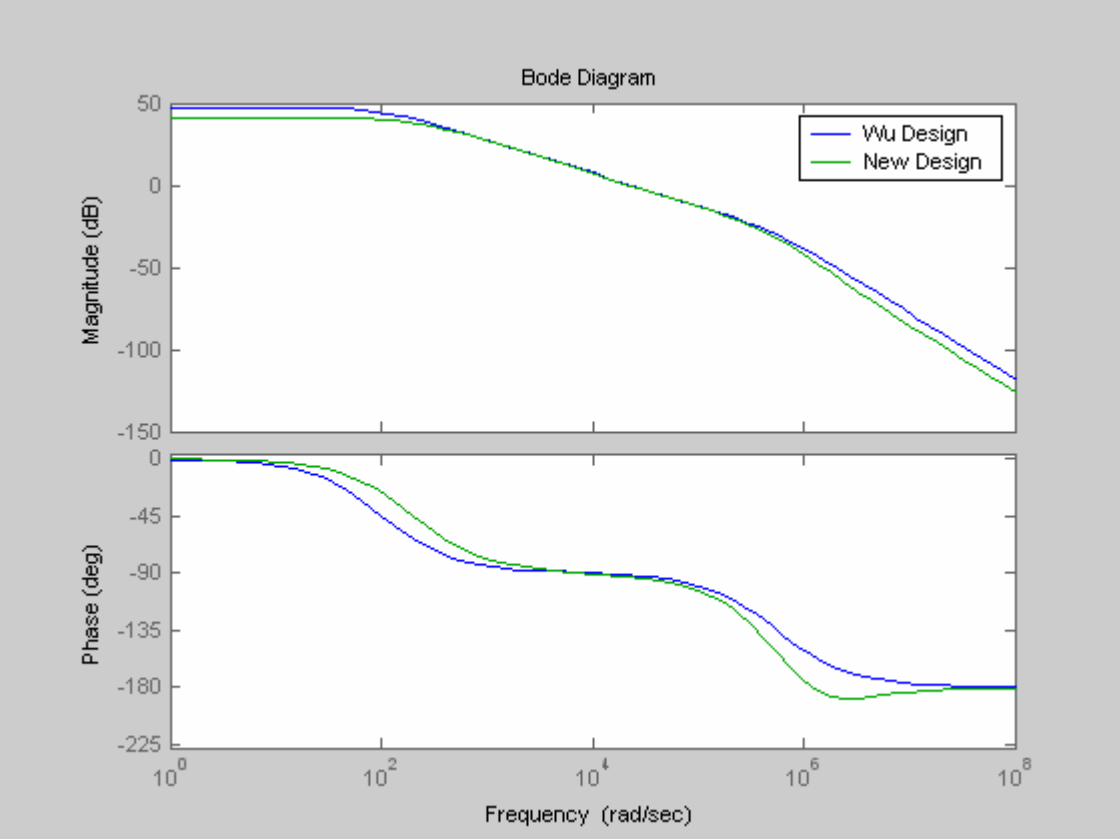

Fig. 21: Inner loop controller comparison

The results for the controllers designed are shown in Figs. 17 to 21.

B. Conclusions

It can be seen from the above results that all specifications are met. In [10] the controllers designed were compared to the outer-inner design and it was shown that the there was significant reduction in the bandwidth of the outer loop controller with the new method proposed compared to the outer-inner design. This implies that the method in [10] gave a better design than the outer-inner design with respect to bandwidth and sensor noise reduction. In this work the controllers designed were compared to those designed in [10]. It is seen in Fig. 20 that G_2 designed using both methods have almost the same bandwidth. The outer loop controller in fact has lower bandwidth than the design in [10].Hence it can be said that this method gives a comparable design to the design in [10],in fact even better which implies that this method is much better the outer-inner

design. Also if compared to the single loop design this method gives a huge reduction in the bandwidth of the outer loop controller just as in the case of the outer-inner design carried out in the usual way. This would help in significant reduction of the sensor noise. The added advantage of this method is that the inner loop design is almost automated. In the case of n number of loops, this automation can prove very beneficial wherein all the inner loops can be automatically designed using the H_∞ method.

CHAPTER V

COMPARATIVE STUDY OF CASCADED DESIGN USING QFT AND H_∞

In this chapter we compare the H_∞ design of a two loop cascade control system with the QFT design.

A. H_∞ Design for a Two Loop Cascade Control Structure

As before a linear time invariant plants having two cascaded sections is considered. The plants have uncertainty which can be of the structured or unstructured form. The plant transfer functions are $P_1(s)=P_{10}(s)+W_1\Delta_1(s)$ and $P_{20}(s)+W_2\Delta_2(s)$ where $W_1(s),W_2(s)$ are additive uncertainty weights and $\|\Delta_1\|_\infty \le 1, \|\Delta_2\|_\infty \le 1$. The reference input to the system is r(t) with corresponding Laplace transform R(s). The design objective is to achieve robust stability along with nominal performance. The LFT form of the control structure is shown in Fig. 22. To solve the problem using the software tools available, this LFT form was converted into the form in Fig. 23 using the method used in [5].

From Fig. 23,

$$z=\begin{bmatrix} z_y \\ z_1 \\ z_2 \\ z_3 \end{bmatrix}, \qquad w=\begin{bmatrix} r \\ d \\ \omega_1 \\ \omega_2 \end{bmatrix}$$

$$y=\begin{bmatrix} e_1 \\ e_2 \\ r \end{bmatrix}, \qquad u=\begin{bmatrix} u_1 \\ u_2 \\ u_3 \end{bmatrix}$$

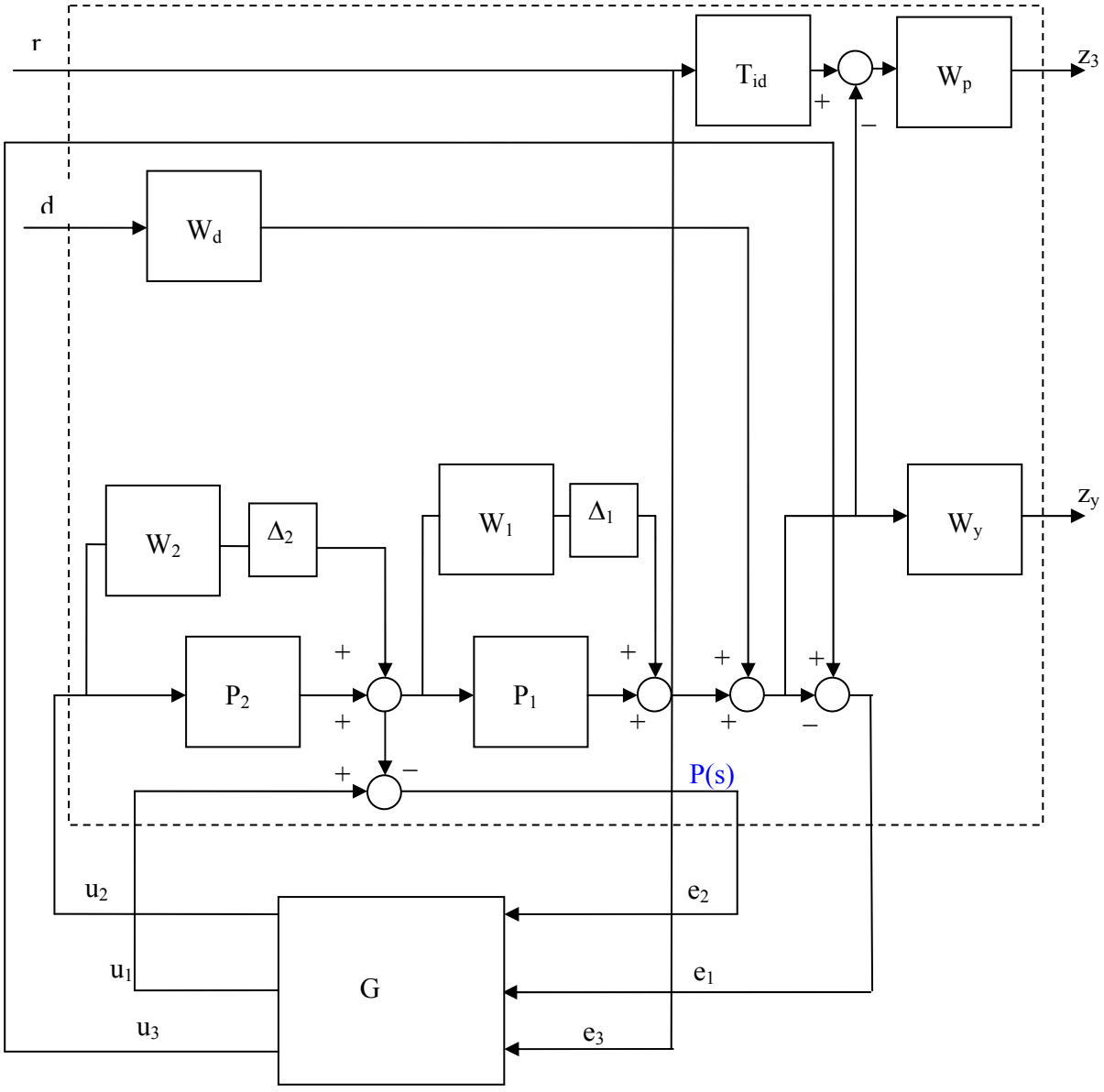

Fig. 22. LFT formulation for two loop control structure

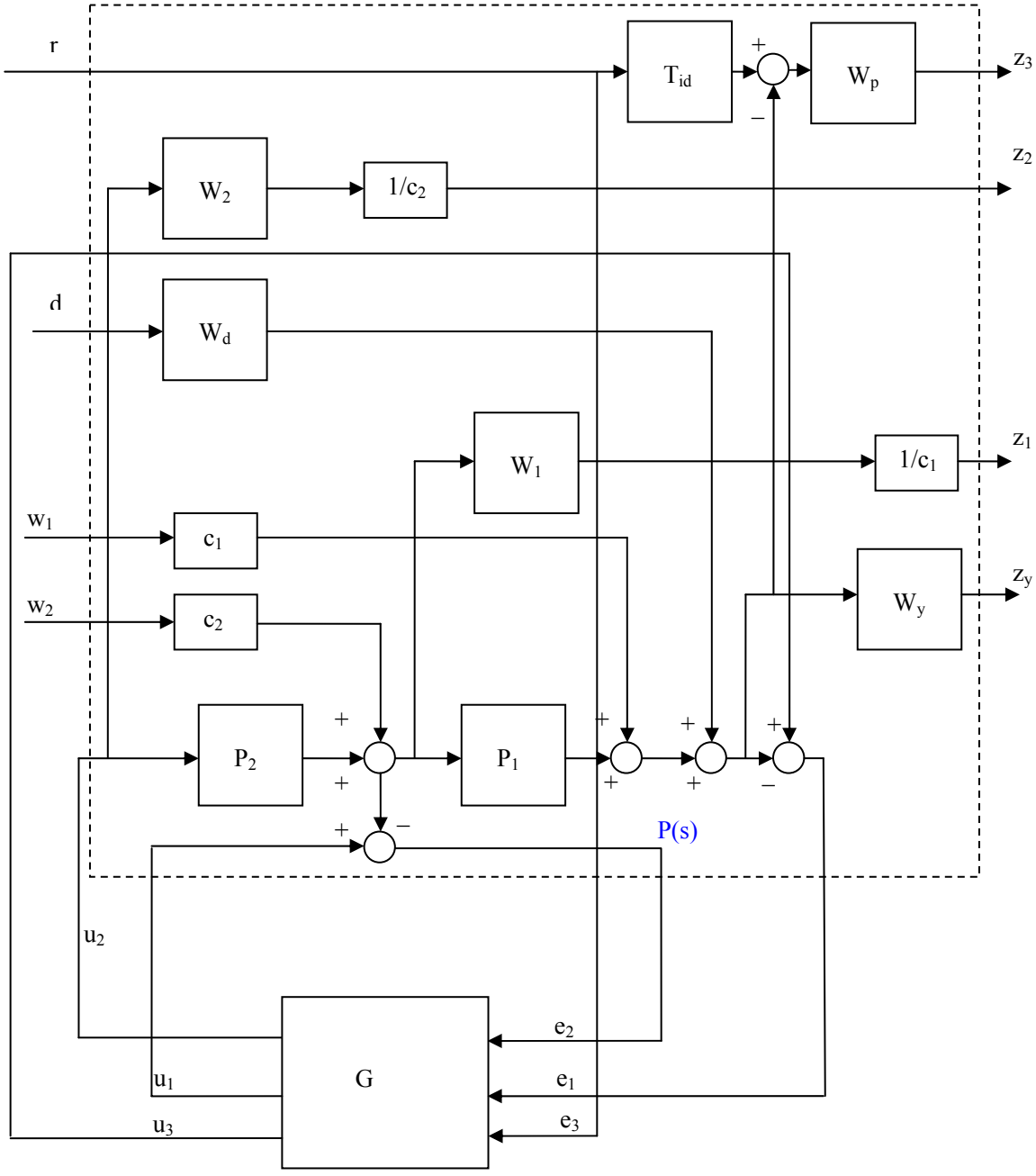

Fig. 23. Modified LFT formulation for two loop control structure

where z, y, w and u are the error variables, measured variables, exogenous inputs and control inputs to the system respectively.

$$P_{zw} = \begin{bmatrix} 0 & W_y W_d & c_1 W_y & c_2 P_1 W_y \\ 0 & 0 & 0 & \dfrac{c_2 W_1}{c_1} \\ 0 & 0 & 0 & 0 \\ T_{id} W_p & -W_d W_p & -c_1 W_p & -c_2 P_1 W_p \end{bmatrix}$$

$$P_{zu} = \begin{bmatrix} 0 & P_1 P_2 W_y & 0 \\ 0 & \dfrac{P_2 W_1}{c_1} & 0 \\ 0 & \dfrac{W_2}{c_2} & 0 \\ 0 & -W_p P_1 P_2 & 0 \end{bmatrix}$$

$$P_{yw} = \begin{bmatrix} 0 & -W_d & -c_1 & -c_2 P_1 \\ 0 & 0 & 0 & -c_2 \\ 1 & 0 & 0 & 0 \end{bmatrix}$$

$$P_{yu} = \begin{bmatrix} 0 & -P_1 P_2 & 1 \\ 1 & -P_2 & 0 \\ 0 & 0 & 0 \end{bmatrix}$$

where P_{zw} ,$P_{zu,}$ P_{yw},P_{yu} are the open loop transfer functions from z to w, z to u, y to w and y to u respectively. W_y, W_p are weights which are to be selected appropriately. T_{id} is the desired closed loop transfer function. W_d shapes the disturbance coming into the system.

$$N_{zw} = P_{zw} + P_{zu} G \left(I - P_{yu} G \right)^{-1} P_{yw}$$

where N_{zw} is the closed loop transfer function from z to w.

The H infinity problem then reduces to minimizing $\|N_{zw}\|_\infty$

B. Design Example

Given:

$$P_{10}(s) = \frac{1}{(s+1)(s+20)}, P_{20}(s) = \frac{1}{(s+1)(s+20)},$$

$$W_1(s)=\frac{0.11}{(s+1)\left(\left(\frac{s}{15}\right)^2+\left(\frac{2\times 0.75\times s}{15}\right)+2\right)},W_2(s)=\frac{0.11}{(s+1)\left(\left(\frac{s}{15}\right)^2+\left(\frac{2\times 0.75\times s}{15}\right)+2\right)}$$

$$W_d(s)=\frac{1}{\left(\left(\frac{s}{5}\right)^2+\left(\frac{2\times 0.75\times s}{5}\right)+1\right)}$$

The weights are taken as

$$W_y=\frac{1}{\left(\frac{s}{25}+1\right)},W_p=\frac{1}{\left(\frac{s}{25}+1\right)},T_{id}=\frac{100}{\left(s^2+10s+100\right)}$$

The $\|N_{zw}\|_\infty$ achieved was 1.6.

The frequency response of the controllers and pre filters designed is shown in Fig. 24.

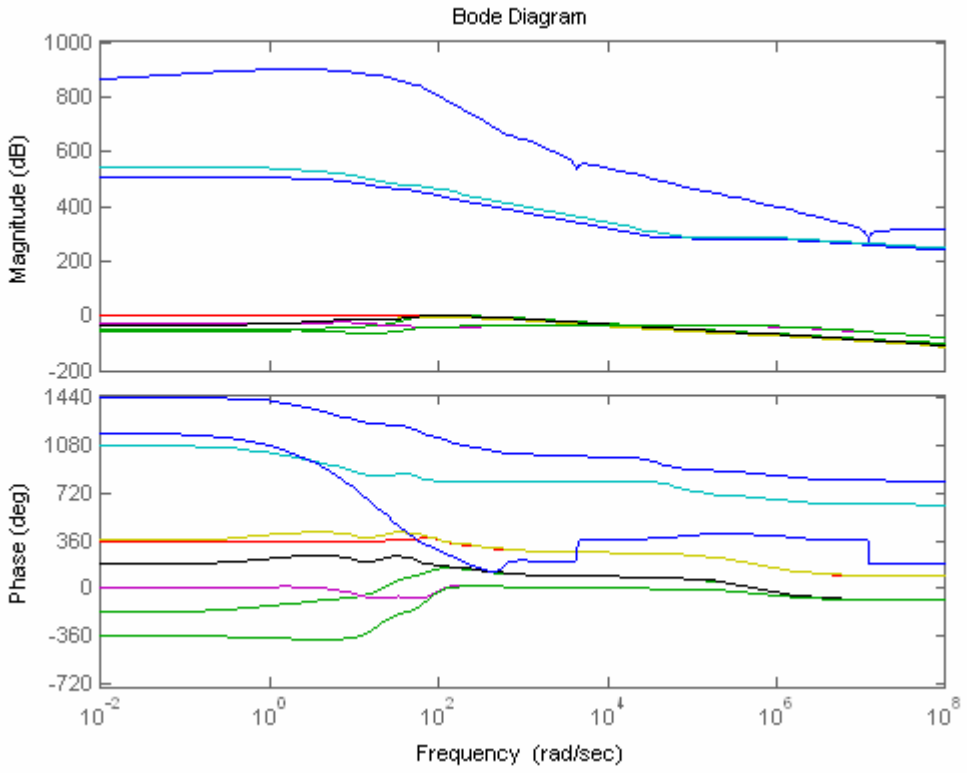

Fig. 24. Frequency response of all prefilters and controllers

C. Conclusions

It can be seen that H_∞ gives a fully populated controller, pre filter matrix. Hence four controllers and five filters are designed using this method. The system has three degrees of freedom. Hence as reasoned out in [11] six of the elements in the nine element controller matrix designed using H_∞ are redundant. The only way the redundancy could be removed is by having the elements of the control matrix diagonal. Also the transfer function between the reference input and output for the control system designed using H_∞ was found out. It included all the nine controllers and pre filters designed. This transfer function was tried to be written in the form $F\left(\frac{P_1G_1P_2G_2}{1+P_2G_2}\right)/\left(1+\left(\frac{P_1G_1P_2G_2}{1+P_2G_2}\right)\right)$ but this was not possible as the corresponding controllers were functions of plants. Hence for bringing two loop H_∞ design on the same platform for comparison with the QFT design we must have the control matrix diagonal. A special class of plants would give such a control matrix but this is yet to be investigated as it would involve a deep insight into the H_∞ design algorithm.

CHAPTER VI

CONCLUSIONS AND FUTURE RESEARCH DIRECTIONS

It has been shown in this thesis that a two loop control structure is not necessary for satisfying typical performance specifications though it finally boils down to a trade off between the various requirements of disturbance rejection, simplicity of controller, noise rejection in the high frequencies etc. . Further the robust outer loop bounds for the inner loop of a two loop control structure has been found analytically. This research could be extended to the generalization of the mapping of outer loop margin condition to inner loop bounds for MIMO systems.

A new method was devised for designing cascade controllers using H_∞ and QFT. It gave better results compared to the outer-inner design and the design in [10]. The added advantage of this method is that the inner loop design is automated. This would be particularly beneficial when there are more than two loops. This can be extended to SISO systems with n loops. Also the H_∞ and QFT designs for a two loop cascade control structure was compared. It was found that two loop cascade design using H_∞ results in redundant controllers and pre filters. Since the only case when QFT and H_∞ can be put on the same platform for comparison is the design with diagonal controllers, a promising research direction could be investigation of a class of plants which result in the H_∞ controllers being diagonal. This could possibly be done by analyzing the algorithm for solving the H_∞ problem.

REFERENCES

1. D.G. Benshabat and Y. Chait, "Application of Quantitative Feedback Theory to a class of missiles," *Journal of Guidance, Control, and Dynamics*, vol. 16, pp. 47-52, 1993.

2. E. Torres, M. Garcia-Sanz , "Experimental results of the variable speed, direct drive multipole synchronous wind turbine TWT1650," *Wind Energy*,vol. 7, pp. 109-118, 2004.

3. I. Horowitz, "Survey of Quantitative Feedback Theory (QFT)," *International Journal of Control*, vol. 53, no. 2, pp. 255–291, 1991.

4. I.M. Horowitz, *Synthesis of Feedback Systems*, Academic Press, New York, 1963.

5. G. Zames, "Feedback and optimal sensitivity: model reference transformations, multiplicative seminorms, and approximate inverse, *IEEE Transactions on Automatic Control*, vol. 26, no. 2, pp. 301-320, 1981.

6. I. Horowitz, and M. Sidi, "Synthesis of cascaded multiple loop feedback systems with large plant parameter ignorance," *Automatica* , vol. 9, pp.589-600, 1973.

7. I. Horowitz and B.C. Wang , "Quantitative synthesis of uncertain cascade feedback systems with plant modification," *International Journal of Control,* vol. 30, no. 5, pp. 837-962, 1979.

8. S. Jayasuriya, and Y. Zhao, "Stability of quantitative feedback designs and the existence of robust QFT controllers," *International Journal of Nonlinear and Robust Control*, vol. 4, pp. 21-46, 1994.

9. M. Lal , S. Jayasuriya , "A comparative study of single loop and multiple loop design for uncertain single input single output systems", in *Proceedings of IMECE'04, 2004 ASME International Mechanical Engineering Congress & Exposition* Anaheim, CA, November 13-19, 2004.

10. W. Wu, and S. Jayasuriya, "A new QFT design method for SISO cascaded-loop design," *Proceedings of the 2000 American Control Conference*, pp. 3827-3831,

June 2000.

11. I. Horowitz, "Fundamental theory of automatic linear feedback control systems," *Automatic Control*, IRE Transactions on , vol. 4, no. 3, pp. 5 – 19, December 1959.

12. R.M.C De Keyser, "Improved mold-level control in a continuous steel casting line", *Control Engineering Practice,* vol. 5, no. 2, pp 231-237, 1997.

13. F. Kong, R.M.C De Keyser ,C. Martien and D. Verhasselt "Model identification for the mold reliable control loop in a continuous casting machine," in *IFAC Symposium on Automation in Mining, Mineral and Metal Processing ,* 1992, pp. 316-321.

14. C. Borghesani, Y. Chait, and O. Yaniv, *Quantitative Feedback Theory Toolbox User's Guide*, The Mathworks Inc., Natick, MA, 1994.

15. J.C. Doyle , K. Glover , P.P. Khargonekar, and B.A. Francis, "State space solutions to standard H_2 and H_∞ control problems", *IEEE Transactions on Automatic Control*, vol. 34, no. 8, pp. 831-847, August 1989.

16. S. Skogestad, and I. Postlethwaite , *Multivariable Feedback Control: Analysis and Design*, John Wiley and Sons, New York, 1997.

17. K.B. Lim, P.G. Maghami, S.M. Joshi, "Comparison of controller designs for an experimental flexible structure," *Control Systems Magazine, IEEE* , vol. 12, no. 3, pp.108 – 118, June 1992.

VITA

Mayank Lal was born on November 26th , 1976 in Jharkhand, India. He received his Bachelor of Technology degree in mechanical engineering from the Indian Institute of Technology (IIT), Kharagpur in June, 1999. In September 2002, he started his M.S. in mechanical engineering at Texas A&M University. His main area of research is robust control.